
Article:
Al Salmi, I.K., Al Mamari, H.H. orcid.org/0000-0003-1684-2010, Robertson, C.C. orcid.org/0000-0002-1419-9618 et al. (7 more authors) (2025) Copper(II) and dioxovanadium(V) complexes based on the antiproliferative chelating agent HDpk44mT: crystallographic analyses, spectroscopic features, and cytotoxicity. ACS Omega, 10 (22). pp. 23440-23460. ISSN 2470-1343

https://doi.org/10.1021/acsomega.5c01984

ACS OMEGA

Open Access

http://pubs.acs.org/journal/acsodf

Article

Copper(II) and Dioxovanadium(V) Complexes Based on the Antiproliferative Chelating Agent HDpk44mT: Crystallographic Analyses, Spectroscopic Features, and Cytotoxicity

Iman K. Al Salmi, Hamad H. Al Mamari, Craig C. Robertson, Makoto Handa, Shohreh Tavajohi, Adam Brookfield, Eric J. L. McInnes, Yoshihito Hayashi, Ebrahim S. Moghadam, and Musa S. Shongwe*

Cite This: *ACS Omega* 2025, 10, 23440−23460

Read Online

ACCESS | Metrics & More | Article Recommendations | Supporting Information

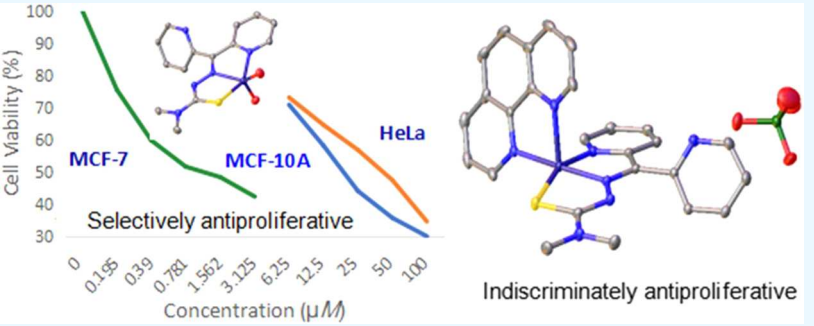

ABSTRACT: Single-crystal X-ray structures of hydrated di(2-pyridyl) ketone 4,4-dimethyl-3-thiosemicarbazone (HDpk44mT·H_2O), the ternary ionic copper(II) complexes [Cu(Dpk-H-44mT)(phen)]$(ClO_4)_2$·1(1/2)MeOH (**1**·1(1/2)MeOH) and [Cu(Dpk44mT)(phen)]ClO_4 (**2**) (Dpk-H-44mT = zwitterionic) form of HDpk44mT; phen = 1,10-phenanthroline and the molecular dioxovanadium(V) complex [VO_2(Dpk44mT)] (**3**) have been determined. Additionally, the solution structures of HDpk44mT·H_2O and complex **3** have been elucidated with the aid of NMR spectroscopic techniques. Coordination compounds **1**·1(1/2)MeOH, **2** and **3** represent extremely rare examples of thiosemicarbazone complexes of their specific kind possessing a *di(2-pyridyl)-ketimine* moiety. Under slightly acidic conditions, complex **1**·1(1/2)MeOH is produced with the thiosemicarbazone ligand occurring in the zwitterionic thio-enolate form, but readily converts to complex **2** in basic medium. In the crystal lattice, these two copper(II) complexes show vastly different patterns of π-π stacking interactions. However, they have in common the ligand-imposed distorted square-pyramidal coordination geometry exhibiting a tetragonally induced disparity between the distances of the axial−equatorial Cu^{II}−N_{phen} bonds. X-band EPR spectroscopy demonstrated retention of the coordination sphere ($g_z > g_{x,y} > 2.00$; $A_z > A_{x,y}$) in frozen solution. The crystallographic asymmetric unit of [VO_2(Dpk44mT)] comprises two discrete molecules, one of which exhibits π-π stacking interactions. Their coordination geometry at the vanadium(V) center is severely distorted square pyramidal. Complexes **1**·1(1/2)MeOH, **2** and **3** are electroactive with reduction potentials lying within the biologically accessible redox potential window. While the copper(II) complexes are highly efficacious as antiproliferative agents against the cancer cell lines HeLa and MCF-7, the main drawback is the lack of selectivity over the normal cell line MCF-10A. In sharp contrast, [VO_2(Dpk44mT)] is specifically and selectively potent toward MCF-7 over HeLa and MCF-10A cells, and may provide impetus for further *in vitro* antitumor investigations.

INTRODUCTION

Thiosemicarbazones constitute a vitally important type of Schiff-base chelating agents having the characteristic structural feature $R^1R^2C{=}N{-}N(H){-}C(=S){-}NR^3R^4$.[1] The relative ease with which these hydrazone ligands can be generated by a one-pot condensation reaction has rendered them a magnet for synthetic researchers in the pertinent fields of chemistry where they find applications. Of structural interest is their coordination versatility deriving from their tendency to undergo base-/metal-assisted tautomerization concomitantly with deprotonation as often demanded by the central metal ion for charge-neutrality of the resultant complex. Moreover, a given polydentate thiosemicarbazone ligand has the ability to exhibit different denticities and coordination modes within the same complex to meet the stereochemical requirements at the

Received: March 3, 2025
Revised: April 25, 2025
Accepted: May 14, 2025
Published: May 28, 2025

metal center.[2−9] Strategic ligand designs involving incorporating moieties bearing additional donor atoms (often pyridyl and/or phenolic rings) can create heterodonor coordination environments[10] for targeted physicochemical and biological activities.[3,8,9,11−27] Steric and electronic effects of substituent groups can be used to modulate or fine-tune physicochemical and pharmacological properties of thiosemicarbazone complexes. There exist a plethora of examples of thiosemicarbazone complexes exhibiting a wide range of pharmacological properties including antitumor,[3,8,9,11−22] antibacterial,[20,21,23] antiviral,[24,25] antifungal[23,26] and antimalarial.[22,27] The discovery that pyridyl-based thiosemicarbazones exhibit marked and selective antiproliferative activity against cancer cells, a property which is enhanced upon complexation with bioactive transition metal ions, has brought these ligands to the forefront of the development of metal-based anticancer drugs.[3,8,9,11−22] Of these ligands, di(2-pyridyl) ketone 4,4-dimethyl-3-thiosemicarbazone (HDpk44mT)[12,13] emerged as the most efficacious antiproliferative agent. Consequently, HDpk44mT and lately di(2-pyridyl) ketone 4-cyclohexyl-4 methyl-3-thiosemicarbazone have featured in groundbreaking cancer research investigations[28−32] particularly those seeking solutions to overcome multidrug resistance. Both thiosemicarbazones exhibit selectivity toward cancer cells over normal cells *in vitro* and *in vivo*.[12,14,17−19]

Single-crystal X-ray structure determinations have shown that, prior to complexation with metal ions, tridentate 2-formylpyridine-,[20,33,34] 2-acetylpyridine-,[15,33,35−38] 2-benzoylpyridine-[14,19,39−41] and di(2-pyridine)-based[7,10,13,42−46] thiosemicarbazones as well as the closely related pyridyl-containing selenosemicarbazone,[47] semicarbazone[48] and aroylhydrazone[49−58] Schiff-base ligands exist either as the *Z* or *E* configurational isomer with respect to the imine bond (Chart S1). In relatively rare cases, these hydrazones can adopt the bifurcated *E′* configuration.[33,48] Invariably, X-ray structures of *di(2-pyridyl) ketimine*-based thiosemicarbazones demonstrate the occurrence of the *Z*-isomer (Chart 1) exhibiting an intramolecular hydrogen bond between the hydrazinic NH group and the nitrogen atom of the adjacent pyridyl moiety.[7,10,13,42−46] Depending on the orientation of the thiocarbonyl group relative to the imine nitrogen [as a consequence of free rotation about the thioamide single bond, *i.e.*, (H)N−C(=S)], the conformation is either *syn,syn* (N_{py}, N_{im} on the same side and N_{im}, S likewise) or *syn,anti* (N_{py}, N_{im} on the same side but N_{im}, S on opposite sides) (Chart 1). When the terminal N^4-position is unsubstituted or monosubstituted (*i.e.*, primary or secondary amino group, respectively), intermolecular H-bonding interactions can lead to formation of dimeric or chain structures.

Chart 1. Illustrations of Crystallographically Determined Conformations of the *Z*-Configuration of Di(2-pyridyl) Ketone Thiosemicarbazones

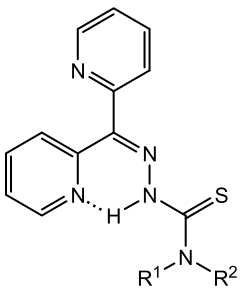

Z(*syn,syn*)

$R^1 = R^2 = CH_3$ (this work)
$R^1/R^2 = N^4,N^4$-(1,4-C_4H_8)[45]
$R^1 = CH_3$, $R^2 = C_6H_5$[46]

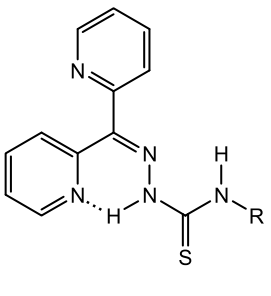

Z(*syn,anti*)

R = H[7,10]; CH_3[13,42]; CH_2CH_3[43]; C_6H_5[44]

In solution, the *E*/*Z* configurational isomers of pyridyl-based hydrazones are readily distinguishable by ^{1}H NMR spectroscopy in that in the *Z*-isomer the hydrazinic proton hydrogen-bonds intramolecularly to the pyridyl nitrogen thereby causing a considerable downfield chemical shift typically in the range ∼14.5−15.9 ppm (cf. ∼10.1−11.9 ppm for the *E*-isomer).[7,15,20,34,36−38,42,48,53−63] Additionally, these pyridyl-based Schiff-base tridentate ligands can adopt different conformational arrangements with the donor atoms (N, N, S/Se/O) positioned *anti* or *syn* relative to one another depending on the relevant σ-bonds rotated (Charts S1 and 1).[7,10,13−15,19,20,33−58] Thiosemicarbazones stabilize predominantly metal ions from the *p*-, *d*- and *f*-blocks;[1] some of the transition-metal thiosemicarbazone complexes exhibit fascinating magneto-structural[64] and catalytic[65] properties among other features. Schiff-base complexes of copper and vanadium tend to be electrochemically active; the copper center shuttles between the +1 and +2 oxidation states (Cu^{II}/Cu^{I} redox couple)[8,16,18,20] whereas the higher-valent vanadium center interconverts among the +3, + 4 and +5 oxidation states (V^{V}/V^{IV} and V^{IV}/V^{III} redox couples).[66] Thiosemicarbazone complexes whose cyclic voltammograms exhibit these redox couples with potentials lying within the biologically accessible redox potential window ranging from −0.4 to +0.8 V *vs* NHE[67] are of pharmacological importance in that they have the ability to generate intracellular reactive oxygen species (ROS) desirable for apoptotic cytotoxicity. High-valent vanadium exists predominantly as oxo-cations: VO^{2+} for the +4 oxidation state (but rarely as the non-oxo V^{4+}ion); VO_2^{+} and VO^{3+} for the +5 oxidation state (but rarely as the non-oxo V^{5+} ion).

Ternary mononuclear complexes of copper(II) and oxovanadium(IV) of the type $[CuL(N,N\text{-donor-L})]^{n+}$[4,9,68−91] and $[VO(L)(N,N\text{-donor-L})]^{n+}$[96,97] [where L represents a neutral or anionic polydentate primary ligand and *N,N*-donor-L stands for a heterocyclic bidentate *N,N*-donor chelating coligand such as 1,10-phenanthroline (phen), 2,2′-bipyridine (bipy), dipyridoquinoxaline (dpq), dipyridophenazine (dppz) or derivatives of these] abound. Such coordination compounds are of considerable interest, not least because of their potential to exhibit DNA binding/cleavage,[71,76,78−81,87,88,90−92,96] anticancer[9,76,80,81,86,90,91,97] and antimicrobial activities.[72−74,77] Some have been explored as models for metallo-enzymes[70,82] while others have been designed to investigate structural and spectroscopic features of interest.[4,69,75,83−85,89,93−95] There is a paucity of ternary copper(II) and oxovanadium(IV) *thiosemicarbazone* complexes of this type; for the former,[4,9,68−76] there exist a mere handful of papers reporting crystallographically characterized examples, and for the latter, none save for a few examples of thiosemicarbazates.[98,99] Even rarer, in the case of the ternary copper(II) complexes, are examples of complexes possessing a pyridyl-based thiosemicarbazone. As far as we are aware, only two papers ever have reported structurally characterized ternary copper(II)-α-pyridyl thiosemicarbazone complexes with phen or bipy (or their substituted derivatives) as coligands: one by Ainscough et al.[75] just over three decades

https://doi.org/10.1021/acsomega.5c01984
ACS Omega 2025, 10, 23440−23460

Scheme 1. Synthetic Routes to the Ternary Copper(II) Thiosemicarbazone Complexes 1 and 2[a]

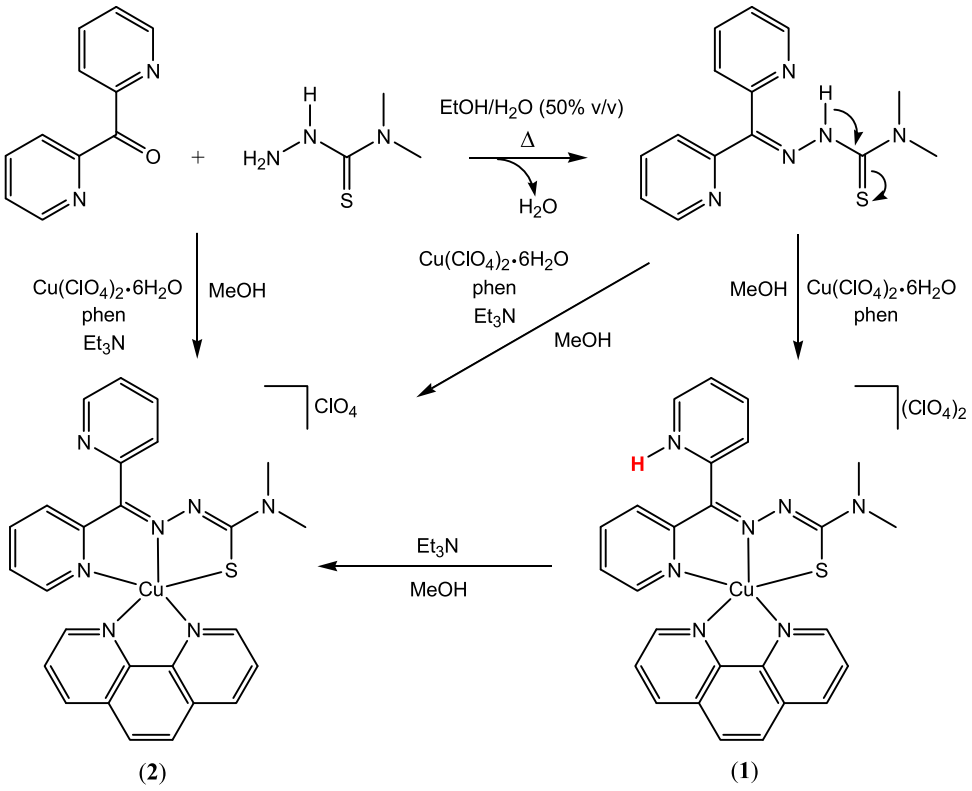

[a]Solvent molecules of crystallization have been omitted.

Scheme 2. Synthetic Routes to the Dioxovanadium(V) Thiosemicarbazone Complex 3

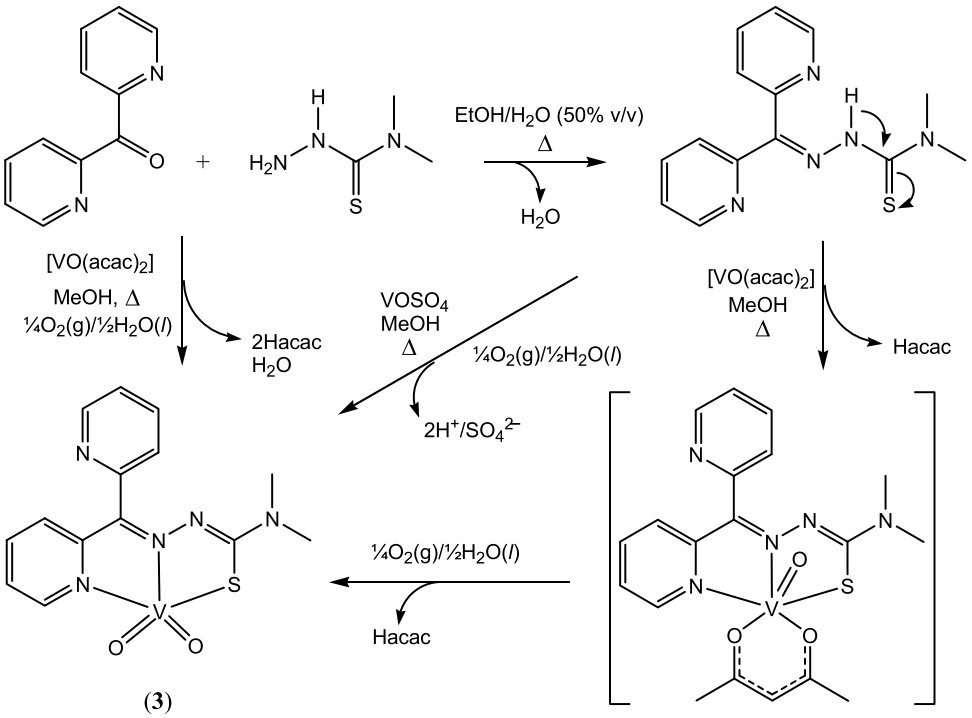

ago based on 2-formylpyridine thiosemicarbazone and the other by Kartikeyan et al.[76] very recently based on 2-formylpyridine 4-phenyl-3-thiosemicarbazone.

In this work, we have produced and crystallographically characterized the *first* examples of ternary copper(II) complexes with a *di(2-pyridyl)*-based thiosemicarbazone, namely [Cu(Dpk-H-44mT)(phen)]$(ClO_4)_2$·1(1/2)MeOH (**1**·1(1/2)MeOH) and [Cu(Dpk44mT)(phen)]ClO_4 (**2**). Moreover, we have also determined the X-ray crystal structure of the thiosemicarbazone HDpk44mT. It is rather surprising

https://doi.org/10.1021/acsomega.5c01984
ACS Omega 2025, 10, 23440−23460

that HDpk44mT has never been employed in the design of this type of ternary copper(II) thiosemicarbazone complexes despite its well-known potent antiproliferative efficacy.[12] Attempts to synthesize the corresponding ternary complex of oxovanadium(IV) afforded the dioxovanadium(V) complex $[VO_2(Dpk44mT)]$ (**3**) instead, which is one of a mere handful of examples of structurally characterized *pyridyl/di(2-pyridyl)*-based thiosemicarbazone complexes of dioxovanadium(V) witnessed by the literature. All three complexes **1**·1(1/2)MeOH, **2** and **3** exhibit fascinating structural and spectroscopic features. The antiproliferative activity of these complexes has been tested against the cancer cell lines MCF-7 (human breast adenocarcinoma) and HeLa (human cervical carcinoma). Moreover, to determine their potential as anticancer metal-based drugs, we have also investigated their cytotoxicity toward the MCF-10A (noncancerous human breast epithelial MCF-10A cell line). In toto, $[VO_2(Dpk44mT)]$ exhibits the most interesting pharmacological properties and lends itself to further exciting *in vitro* anticancer investigations.

RESULTS AND DISCUSSION

Syntheses and Identification of Copper(II) and Dioxovanadium(V) Complexes of HDpk44mT. The thiosemicarbazone ligand (HDpk44mT) was produced straightforwardly by the acid-catalyzed Schiff-base condensation reaction in accordance with a synthetic procedure described in the literature.[13] That it was isolated with a water molecule of crystallization was demonstrated by microanalysis and, subsequently, verified definitively by structural analysis. Its existence in the thioamide (thione) tautomeric form as a pure solid substance, having the characteristic −N(H)−C(=S)− functional feature, was evidenced by the ν(N−H) and ν(C=S) absorption bands at 3450 and 1002 cm^{-1}, respectively, coupled with the absence of the thio-enol S−H stretch around 2600 cm^{-1}.[10] The Schiff-base imine absorption band was observed at 1655 cm^{-1}. Selected portions of the IR spectrum of this ligand along with those of its complexes are displayed in Figure S1. Illustrative representations of the synthetic routes to the mononuclear copper(II) complexes $[Cu(Dpk\text{-}H\text{-}44mT)(phen)](ClO_4)_2$·1(1/2)MeOH (**1**·1(1/2)MeOH) and $[Cu(Dpk44mT)(phen)]ClO_4$·*x*MeOH (**2**·*x*MeOH) and the dioxovanadium(V) complex $[VO_2(Dpk44mT)]$ (**3**) are given in Schemes 1 and 2, respectively. The formation of complex **1**·1(1/2)MeOH having the zwitterionic (dipolar) ligand was facilitated by the slightly acidic reaction conditions; in contrast, in basic medium the reaction favored complex **2** with the ligand in the thioenolate (thiolate) form. Pertaining to complex **1**·1(1/2)MeOH, protonation of a non-hydrogen-bonded pyridyl moiety in closely related thiosemicarbazones at pH ≤ 7 has been demonstrated crystallographically[7,13,35,40] in previous studies. Under basic conditions, complex **1**·1(1/2)MeOH is readily converted to complex **2** which is isolated with a MeOH molecule of crystallization (*i.e.*, **2**·MeOH). Interestingly, as demonstrated crystallographically, when prepared from the ligand rather than from complex **1**·1(1/2)MeOH, complex **2** is obtained nonsolvated. Both **1**·1(1/2)MeOH and **2** (or **2**·MeOH) were isolated from their solutions in MeOH as large black blocks and the results of their CHN analyses are consistent with the proposed chemical formulas. Moreover, that they are ionic was proven by the electrical conductivity of their solutions (10^{-3} M) in common organic solvents:[100] the former is a 2:1 electrolyte type [Λ_M (Ω^{-1} cm^2 mol^{-1}): 86 (EtOH), 165 (DMF) and 192 (MeOH)] whereas the latter is a 1:1 electrolyte type [Λ_M (Ω^{-1} cm^2 mol^{-1}): 38 (EtOH), 84 (DMF) and 118 (MeOH)]. The positive-ion electrospray ionization (ESI) mass spectra of complexes **1**·1(1/2)MeOH and **2** are identical implying dissociation of the pyridinium N−H bond of **1**·1(1/2)MeOH in this process. As can be seen from Figure S2, the representative mass spectrum exhibits the parent peak at m/z = 527 ascribable to the complex cation $[Cu(Dpk44mT)(phen)]^+$, and having an isotopic distribution pattern closely matching the simulated one. Fragmentation involving the loss of the phen coligand results in the formation of the ion $[Cu(Dpk44mT)]^+$ associated with the peak at m/z = 347.

For the synthesis of $[VO_2(Dpk44mT)]$ (**3**) either $[VO(acac)_2]$ or $VOSO_4$ (Scheme 2) can be utilized as the source of the vanadyl ion which is subsequently oxidized and oxygenated to the dioxovanadium(V) ion. In the case of the former, mechanistically, the reaction is expected to commence with attachment of the thiosemicarbazone to the coordinatively unsaturated $[VO(acac)_2]$ complex through the thione sulfur atom, as crystallographically demonstrated in the closely related semicarbazone complex $[VO(H2APS)(acac)_2]$ (H2APS = 2-acetylpyridine semicarbazone)[101] in which the keto oxygen is attached to the vanadium atom of $[VO(acac)_2]$ at the vacant site; though rare, the occurrence of similar monodentate coordination of a thiosemicarbazone ligand has been shown structurally in the complexes $[M(Ap4Et)(H_2ApEt)]$ (M = Pd^{II}, Pt^{II}; H_2Ap4Et = 2′-hydroxyacetophenone 4-ethyl-3-thiosemicarbazone).[2] Thereafter, upon tautomerization and deprotonation, the thiosemicarbazone is expected to coordinate tridentately (Scheme 2)[102−104] with concomitant displacement of one of the acetylacetonate ligands to afford the intermediate complex "[VO(Dpk44mT)(acac)]" (observed in solution in an inert atmosphere), an analogue of several crystallographically characterized complexes of closely related ligand systems.[103,105−107] Under aerobic conditions, the reaction proceeds to generate the air-stable complex $[VO_2(Dpk44mT)]$ (**3**) as shiny orange blocks whose solution in organic solvents is nonelectrolytic, as expected. This dioxovanadium(V) complex has been formulated in accordance with CHN analysis and ESI-MS (molecular peak: m/z = 367). It is noteworthy that attempts to synthesize the nonexistent complex "$[VO(Dpk44mT)(phen)]ClO_4$", the oxovanadium(IV) analogue of **2**, in the presence of ClO_4^- as a possible counteranion were futile; complex **3** was produced instead and this was proven conclusively by single-crystal X-ray crystallography.

All three complexes **1**·1(1/2)MeOH, **2** and **3** are readily identifiable by Fourier transform infrared (FT-IR) spectroscopy. Selected portions of the IR spectra are displayed in Figure S1. The disappearance of the ligand N−H absorption band and the shift of the thione C=S absorption band to 853, 845, and 823 cm^{-1}, respectively, are indicative of thione-thioenol tautomerization. As evident from Figure S1(a), there is a marked shift of the stretching frequency of the imine bond upon coordination of the ligand imine nitrogen donor atom to the central metal ions [ν(C=N) = 1622, 1622, and 1598 cm^{-1} for **1**·1(1/2)MeOH, **2** and **3**, respectively]. Conspicuously, in the FT-IR spectra of the copper(II) complexes are intense absorption bands of the ClO_4^- counterions in the range 1121−1088 cm^{-1} accompanied by a weaker one around 624 cm^{-1}.[108−111] An overlay of the IR spectra of HDpk44mT

https://doi.org/10.1021/acsomega.5c01984
ACS Omega 2025, 10, 23440−23460

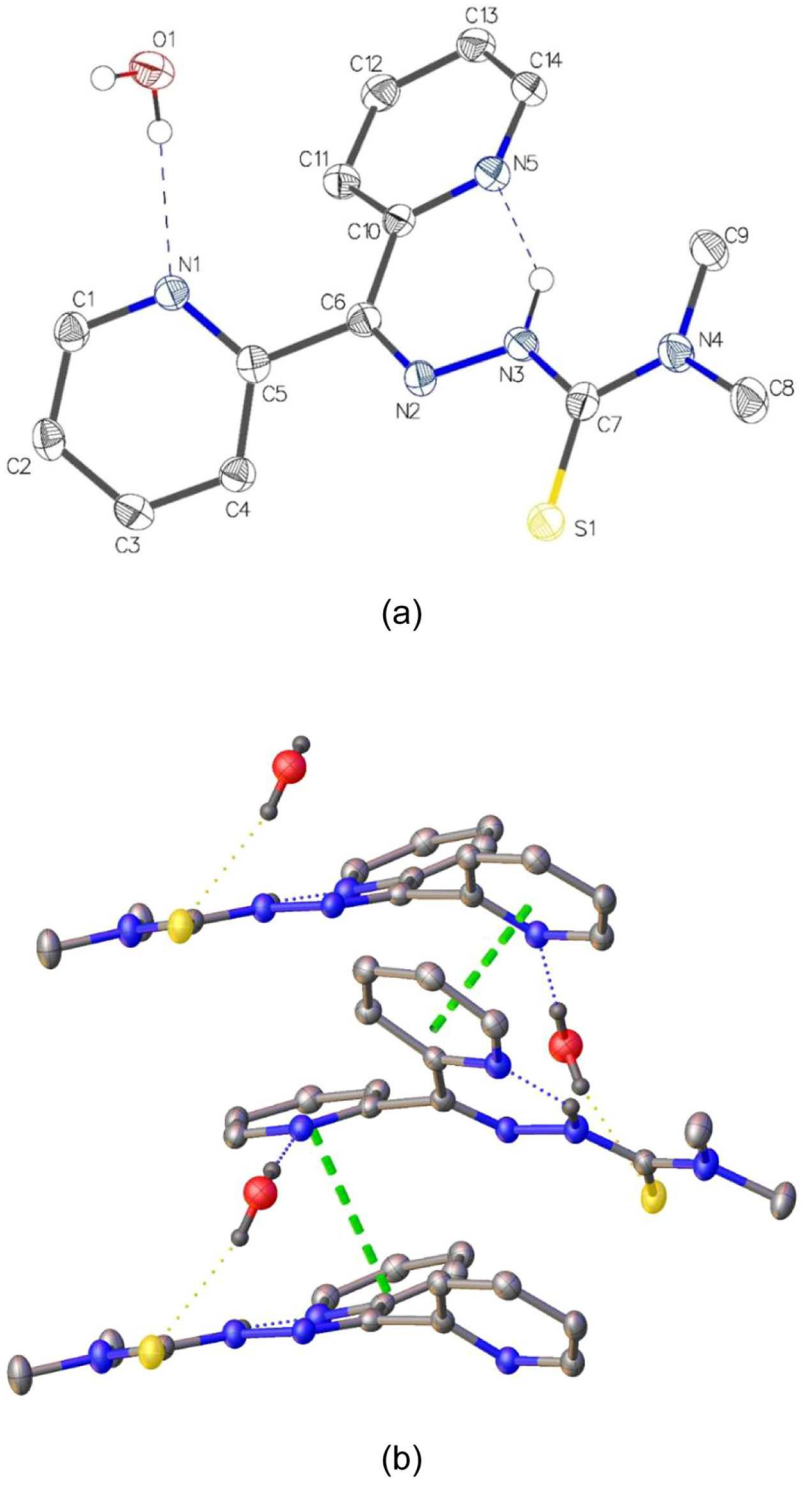

Figure 1. X-ray crystal structure of HDpk44mT·H_2O: (a) crystallographic asymmetric unit, (b) a portion of a chain of thiosemicarbazone molecules with intervening water molecules of crystallization.

and $[VO_2(Dpk44mT)]$ in Figure S1(b) shows prominent absorption bands at 956, 934, and 919 cm^{-1} along with a shoulder at 913 cm^{-1}, characteristic of $\nu_{as}(VO_2)$ and $\nu_s(VO_2)$,[101,102,112−116] and attributable possibly to two independent complex molecules as revealed by single-crystal X-ray analysis. The oxidation states of the copper and vanadium atoms in the coordination spheres of these complexes were inferred from the established chemical formulas as +2 and +5, respectively, and subsequently verified by room-temperature (RT) magnetic susceptibility measurements. The values of effective magnetic moment, $[\mu_{eff} = (8\chi_M T)^{1/2}]$, for the complexes [Cu(Dpk-H-44mT)(phen)]-$(ClO_4)_2$·1(1/2)MeOH and $[Cu(Dpk44mT)(phen)]ClO_4$ are 1.78 and 1.73 μ_B, respectively, and compare favorably with the value of μ_S, $[4S(S + 1)]^{1/2}$, for a single unpaired electron, in accord with the $[Ar]3d^9$ ground-state electron configuration of the central metal atom. Moreover, these RT values of μ_{eff} lie within the range (μ_{eff} = 1.7 − 2.2 μ_B) reported in the literature

https://doi.org/10.1021/acsomega.5c01984
ACS Omega 2025, 10, 23440−23460

for closely related mononuclear complexes.[82,84,93,94] [VO_2(Dpk44mT)] is diamagnetic on account of the 3*d*-subshell of the vanadium(V) ion being vacant.

Single-Crystal X-ray Crystallography. The X-ray crystal structure determinations of HDpk44mT·H_2O and complexes **1**·1(1/2)MeOH, **2** and **3** were performed using diffraction data collected at LT (100 or 110 K). All atoms but hydrogen were refined anisotropically. Hydrogen atoms were placed in calculated positions with idealized geometries [aromatic sp^2 C−H = 0.95 Å and aliphatic ($-CH_3$) sp^3 C−H = 0.98 Å] and then refined by employing a riding model and isotropic displacement parameters [$U_{iso}(H) = 1.2U_{eq}(C_{sp^2})$ or $1.5U_{eq}(C_{sp^3})$ and O]. The values of the final R_1 index [$I \geq 2\sigma(I)$] for HDpk44mT·H_2O and complexes **1**·1(1/2)MeOH, **2** and **3** are 3.29, 5.32, 3.89 and 4.43%, respectively. The crystal data and parameters for data collection and structure refinement are compiled in Table S1.

X-ray Analysis of HDpk44mT·H_2O. The thiosemicarbazone ligand HDpk44mT crystallized in the orthorhombic $P2_12_12_1$ space group with $Z = 4$, and the crystallographic asymmetric unit shows the presence of a water molecule of crystallization (Figure 1). Indeed, as expected of a di(2-pyridyl)-based thiosemicarbazone (Chart 1), this ligand exists in the *Z*-isomeric form, and the *syn-syn* orientation of the donor atoms relative to one another is consistent with the N^4-terminal amino group being tertiary. The *Z* configuration causes intramolecular hydrogen bonding between the pyridyl and hydrazinic moieties adjacent to each other (Figure 1). Crystal packing shows one-dimensional (1D) chains of molecules of HDpk44mT linked by water molecules through intermolecular H-bonding interactions involving the nitrogen atom of the second pyridyl ring of one ligand molecule and the thiocarbonyl sulfur of the next ligand molecule [Figures 1b and S3]. The H-bonding parameters are presented in Table 1.

Table 1. H-Bonding Parameters and Selected Bond Distances and Angles for HDpk44mT·H_2O[a]

hydrogen-bond geometry (Å, °)				
D*−H···*A	***D*−H**	**H···*A***	***D*···*A***	***D*−H···*A***
N3−H3···N5	0.93(3)	1.80(3)	2.598(3)	143(3)
O1−H1A···N1	0.82(5)	2.07(5)	2.883(3)	173(4)
O1−H1B···S1[1]	0.86(4)	2.48(4)	3.329(3)	167(3)
bond distances (Å) and angles (°)				
C5−C6	1.498(3)	C6−N2	1.300(3)	
N2−N3	1.362(3)	C7−N3	1.369(4)	
C7−S1	1.683(3)	C7−N4	1.345(4)	
C8−N4	1.462(3)	C9−N4	1.469(4)	
C6−N2−N3	118.1(2)	C10−C6−C5	119.5(2)	
N3−C7−S1	123.5(2)	N4−C7−S1	123.1(2)	

[a]Symmetry code (1): 1/2 + *x*, 1/2 − *y*, 1 − *z*.

Each chain is stabilized by $\pi-\pi$ stacking interactions between the intermolecularly H-bonded pyridyl ring (plane N1/C1−C5) of one molecule and the intramolecularly H-bonded pyridyl ring (plane N5/C10−C14) of the next molecule [1/2 + *x*, 1/2 − *y*, 1 − *z*, centroid-centroid distance 3.7134(15) Å, shift distance 1.562(4) Å, angle 6.64(9)°] (Table S2).

The distance of the imine bond [C6−N2 = 1.300(3) Å] is comparable with those reported for other hydrazones (C═N: 1.26−1.30 Å).[7,9,10,13−15,19,20,33−58] NB: In the reduction of 2-acetylpyridine 4,4-dimethyl-3-thiosemicarbazone, the resultant C−N single bond was ∼1.47 Å.[38] That HDpk44mT was isolated as the thione (thio-keto) tautomer, as is usually the case for thiosemicarbazones, is demonstrated by the thioamide carbon−sulfur bond length [C7−S1 = 1.683(3) Å] which lies within the literature range 1.65−1.70 Å.[7,9,10,13−15,19,20,33−58] The distances of the backbone chemical bonds N2−N3, N3−C7 and C7−N4 are normal for uncoordinated thiosemicarbazones. The selected bond angles shown in Table 1 are consistent with the orbital hybridizations for the pertinent central atoms.

*X-ray Analyses of **1**·1(1/2)MeOH and **2**.* Both [Cu(Dpk-H-44mT)(phen)]$(ClO_4)_2$·1(1/2)MeOH (**1**·1(1/2)MeOH) and [Cu(Dpk44mT)(phen)]ClO_4 (**2**) crystallized in the monoclinic space group $P2_1/n$ with $Z = 4$. The asymmetric unit of **1**·1(1/2)MeOH comprises the complex cation [Cu(Dpk-H-44mT)(phen)]$^{2+}$ with the noncoordinated pyridyl moiety protonated, two perchlorate counterions and one-and-a-half methanol solvent molecules of crystallization. As depicted in Figure 2, the pyridinium ring is hydrogen-bonded to a methanol molecule (N−H···O) which in turn interacts with a perchlorate ion by H-bonding (O−H···O). The pyridinium ring also interacts with the other perchlorate counterion and the methanol molecule with half occupancy through weak nonclassical H-bonds (Table S3). Crystal packing shows $\pi-\pi$ stacking interactions between the coordinated pyridyl rings (plane: ring atoms N1,C1−C5) of adjacent complex cations [Figure 2b] with a centroid-centroid distance of 3.950(3) Å, shift distance of 1.669(6) Å and angle of 0.000(11)° (Table S2).

The asymmetric unit of complex **2** consists of the complex cation [Cu(Dpk44mT)(phen)]$^+$ and a perchlorate counteranion [Figure 3a]. In contrast to **1**·1(1/2)MeOH, **2** exhibits $\pi-\pi$ stacking interactions between phen coligands of adjacent complex cations involving all three phen rings [Figure 3b] with intercentroid distances in the range 3.5462−3.9564 Å (Table S2).

In the complex cations of **1**·1(1/2)MeOH and **2**, the tridentate thiosemicarbazonate ligand and bidentate coligand are oriented virtually orthogonally with respect to each other thereby adopting meridional and axial−equatorial coordination modes, respectively, to afford a five-coordinate geometry at the metal center. The angle of tilting of the uncoordinated pyridyl moiety off perpendicularity, which is 33.5(3)° in **1**·1(1/2)MeOH and 32.27(9)° in **2**, was determined from the torsion angle of the C5−C6−N2 and C10−C14,N5 planes, which is 56.50(3)°in **1**·1(1/2)MeOH and 57.73(9)°in **2**. Selected bond distances and angles for both complexes are presented in Table 2. The Schiff-base imine bonds exhibit characteristic distances [C6−N2 = 1.302(4) and 1.301(3) Å] in **1**·1(1/2)MeOH and **2**, respectively, comparable with those encountered in the literature (1.27−1.32 Å).[9,33,117,118] The lengths of the bonds in the ligand backbone N2−N3−C7-N4 are indicative of significant delocalization of π-electrons. That the thiosemicarbazone ligand has tautomerized and deprotonated is evidenced by the magnitude of the carbon−sulfur bond distances [C7−S1 = 1.740(3) and 1.748(2) Å in **1**·1(1/2)MeOH and **2**, respectively],[9,33,117,118] which is consistent with single-bond character of the thioenolate carbon−sulfur bond and much longer than that of the thiocarbonyl bond [C7−S1 = 1.683(3) Å] of the free thione ligand HDpk44mT.

It can be deduced from the values of the trigonality index [$\tau = (\beta - \alpha)/60°$][119] for **1**·1(1/2)MeOH and **2** (0.28 and 0.24, respectively) that the coordination spheres are distorted square pyramidal [τ = 0 and 1 for idealized square pyramidal and

https://doi.org/10.1021/acsomega.5c01984
ACS Omega 2025, 10, 23440−23460

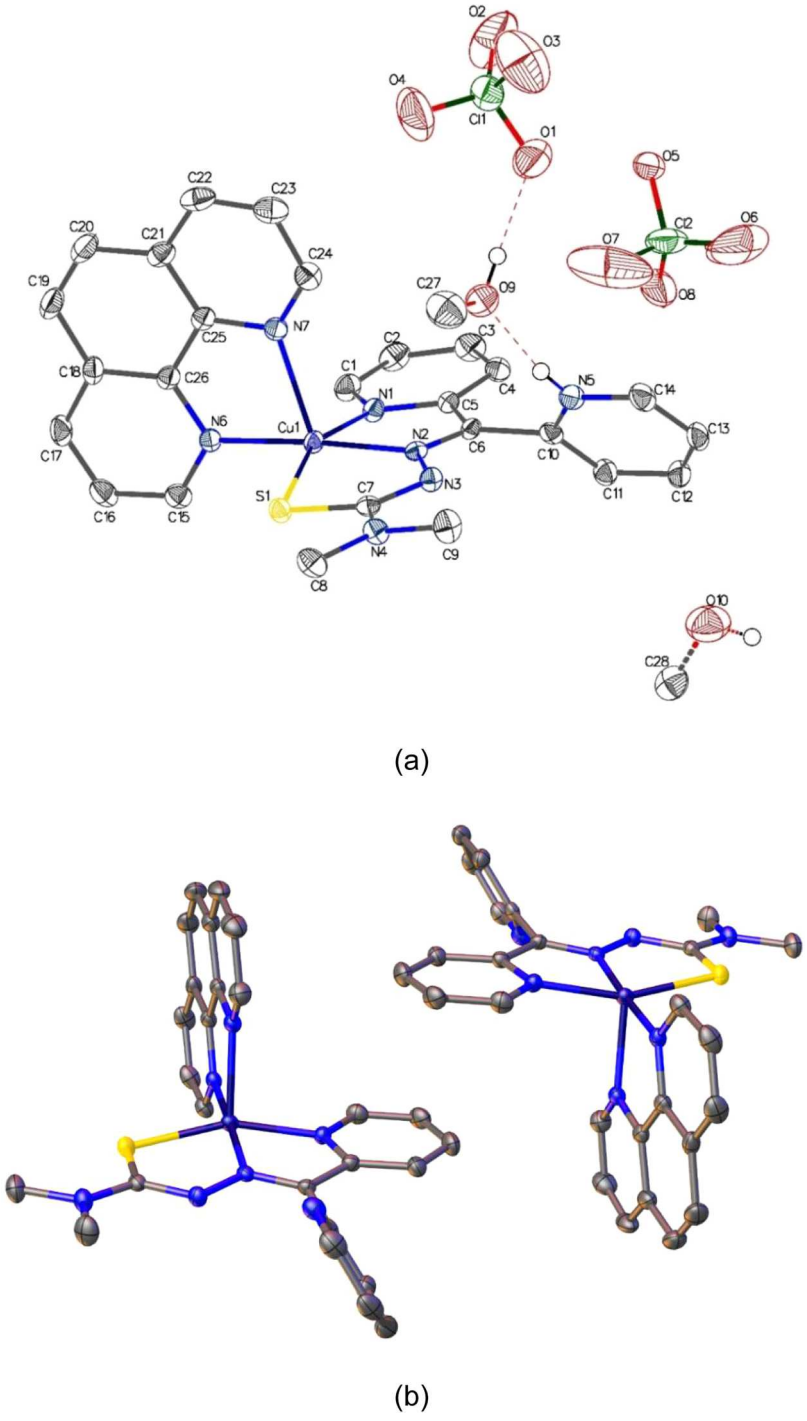

Figure 2. X-ray crystal structure of [Cu(Dpk-H-44mT)(phen)]$(ClO_4)_2$·1(1/2)MeOH (**1**·1(1/2)MeOH): (a) crystallographic asymmetric unit and (b) $\pi-\pi$ stacking interaction.

trigonal bipyramidal coordination geometries, respectively]. The pyridyl nitrogen, imine nitrogen and thioenolate sulfur of the tridentate thiosemicarbazone ligand together with one of the phen pyridyl nitrogens define the equatorial plane, out of which the central metal ion is displaced 0.1772(12) Å in **1**·1(1/2)MeOH and 0.1723(9) Å in **2** toward the second phen nitrogen donor atom which is apically positioned. This coordination sphere implies that in the ground state, of the copper(II) 3*d*-orbitals, the $d_{x^2-y^2}$ orbital has the highest energy, hence singly occupied. Conspicuously, there exists a disparity between the $Cu^{II}-N_{phen}$ coordinate bonds, the axial one being considerably longer [2.203(3) *vs* 2.009(3) Å in **1**·1(1/2)MeOH and 2.2091(19) *vs* 2.0147(18) Å in **2**]. This asymmetric coordination of phen and the closely related ligands bipy and dpq, along with their derivatives, is a characteristic feature of square pyramidal[9,68−80,82−89] and octahedral[81,90] copper(II) complexes in which this heterocyclic symmetrical bidentate ligand adopts an axial−equatorial coordination arrangement. As observed in the distorted octahedral structures of $[Cu(phen)_3](ClO_4)_2$,[120] [Cu(tdp)(phen)]ClO_4[81] (where Htdp = 2-[(2-(2-hydroxyethylamino)ethylimino)methyl]phenol) and [Cu(trien)(bipy/phen)]-

https://doi.org/10.1021/acsomega.5c01984
ACS Omega 2025, 10, 23440−23460

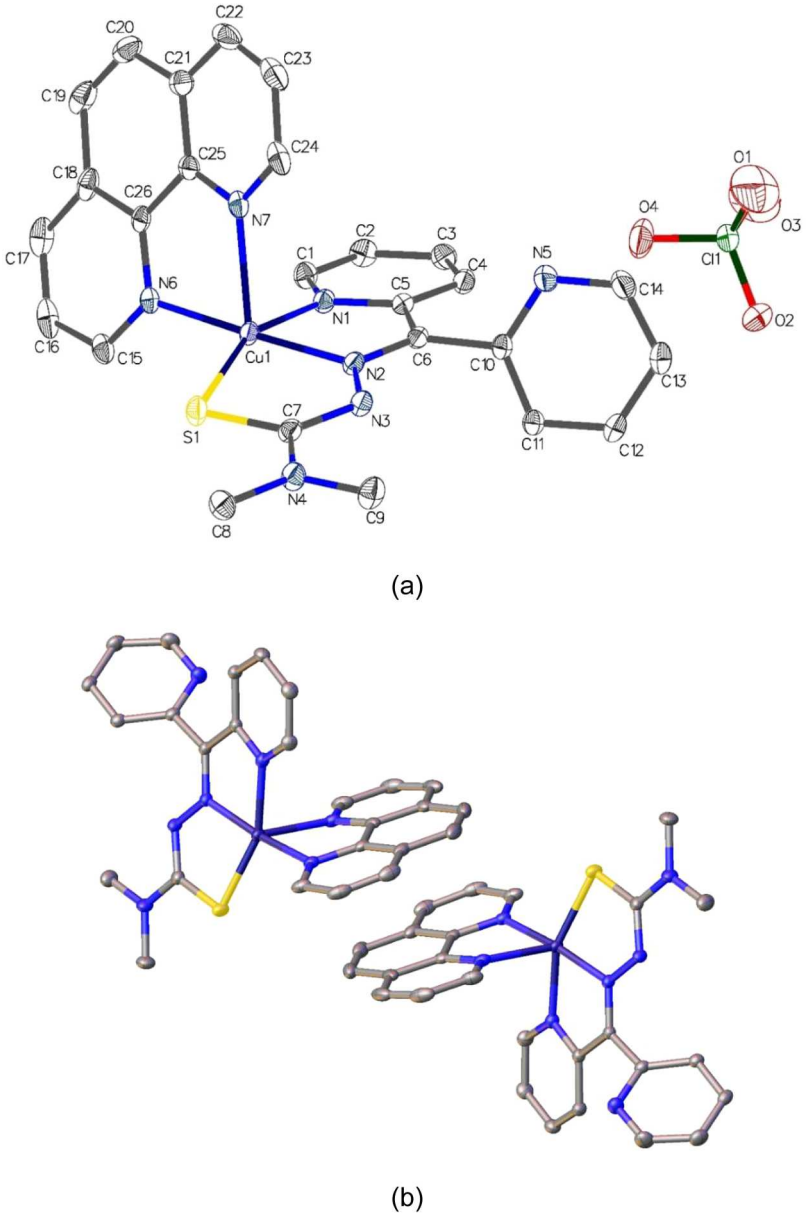

Figure 3. X-ray crystal structure of $[Cu(Dpk44mT)(phen)]ClO_4$ (**2**): (a) crystallographic asymmetric unit and (b) $\pi-\pi$ stacking interaction.

$(ClO_4)_2$[90] (where trien = triethylenetetramine), the axial Cu−N bond of the coligand which lies along the Jahn−Teller axis is considerably weakened. Likewise, invariably, square pyramidal ternary copper(II) complexes[9,68−80,82−89] with the heterocyclic bidentate ligand in an axial−equatorial coordination mode exhibit this structural feature. The magnitude of the difference between the two Cu−N bond distances of the coligand, Δd(Cu−N), is typically 0.17−0.35 Å.[9,68−90] However, if the same bidentate ligand, namely phen, coordinates equatorially[91−95] or occurs in a trigonal bipyramidal coordination geometry, as in the complex $[Cu\{N(CN)_2\}(phen)_2]^+$,[121] the two Cu−N bonds are virtually of equal distance since such copper(II) complexes are not subject to the Jahn−Teller effect. The tetragonal elongation of one of the two Cu−N_{phen} bonds leads to a decrease in the N−Cu^{II}−N bite angle with values ranging from 75 to 79°[9−90,120] whereas the corresponding angles not affected by the Jahn−Teller distortion are reliably in the range 80−82°.[91−95,121] In complexes **1**·1(1/2)MeOH and **2**, the values of $\Delta d(Cu-N)_{phen}$ are the same (0.194 and 0.1944 Å, respectively) and the phen N−Cu^{II}−N bite angles are 79.49 and 78.80°, respectively. Incidentally, that the Jahn−Teller effect can impose a square pyramidal geometry on a binary bis(chelate) copper(II) complex possessing a potentially tridentate ligand is exemplified by the X-ray crystal structure of $[Cu(Dpk44mT)_2]$[122] in which the ligand exhibits different denticities.

X-ray Analysis of ***3****.* There exist a number of mononuclear dioxovanadium(V) complexes possessing a diverse range of ligands. However, papers reporting crystallographically characterized dioxovanadium(V) complexes of *pyridyl*[102,104,105,123−125] or *di(2-pyridyl)*[117] *thiosemicarbazones* are few and far between. $[VO_2(Dpk44mT)]$ crystallized in the triclinic space group P with Z = 4. In the asymmetric unit reside two crystallographically discrete molecules, designated A and B (Figure 4), which are similar but not identical. That the thiosemicarbazone ligand underwent tautomerization followed by deprotonation is evidenced by the typical thioenolate C−S^- bond distances of 1.746(3) and 1.759(2) Å (Table

https://doi.org/10.1021/acsomega.5c01984
ACS Omega 2025, 10, 23440−23460

Table 2. Selected Bond Distances (Å) and Angles (°) for [Cu(Dpk-H-44mT)(phen)]$(ClO_4)_2$·1(1/2)MeOH (**1**·1(1/2)MeOH) and [Cu(Dpk44mT)(phen)]ClO_4 (**2**)

	1·1(1/2)MeOH	**2**
Cu1−S1	2.2680(9)	2.2682(7)
Cu1−N1	2.026(3)	2.0590(19)
Cu1−N2	1.970(3)	1.9625(18)
Cu1−N6	2.009(3)	2.0147(18)
Cu1−N7	2.203(3)	2.2091(19)
C7−S1	1.740(3)	1.748(2)
C6−N2	1.302(4)	1.301(3)
N2−N3	1.347(4)	1.353(2)
C7−N3	1.354(4)	1.341(3)
C7−N4	1.327(4)	1.339(3)
N1−Cu1−S1	158.91(8)	158.04(5)
N1−Cu1−N7	97.50(11)	89.50(7)
N2−Cu1−S1	83.99(8)	84.54(5)
N2−Cu1−N1	81.13(11)	80.28(7)
N2−Cu1−N6	175.94(11)	172.29(7)
N2−Cu1−N7	104.56(11)	102.43(7)
N6−Cu1−S1	95.14(8)	102.32(5)
N6−Cu1−N1	98.65(11)	92.15(7)
N6−Cu1−N7	79.49(11)	78.80(7)
N7−Cu1−S1	100.66(8)	109.31(5)

3).[9,33,102,104,105,116−118] In the crystal lattice, the complex molecules are packed such that only molecule B engages in π-π stacking interactions, involving the coordinated pyridyl ring, with a symmetry equivalent of itself [plane: N1B,C1B−C5B, symmetry code: $-x$, $1-y$, $1-z$; centroid-centroid separation = 3.4025(19) Å, shift difference = 0.483(4) Å and shift angle = 0.00(17)°] (Table S2).

The five-coordinate geometry at the metal center arises from the equatorial tridentate coordination of the thioenolate ligand $[Dpk44mT]^-$ and the axial−equatorial coordination of the vanadyl oxygen atoms. In molecules A and B, the uncoordinated pyridyl moiety is tilted 32.82(9) and 39.51(9)°, respectively, off perpendicularity as determined from the torsion angle of the planes of C5−C6−N2 and C10−C14,N5 [57.18(9) and 50.49(9)°, respectively]. The values of the angular distortion parameter [τ = 0.091 and 0.050 for molecules A and B, respectively][119] point to a distorted square pyramidal coordination geometry, taken at face value; however, as is always the case with such dioxovanadium(V) complexes, the bond angles β and α deviate considerably from linearity (Table 3).[101,102,104,105,112−117,123] The vanadium(V) atoms V1A and V1B are displaced out of the mean basal plane by 0.5170(11) and 0.529(1) Å, respectively, toward the apical oxygen donor atom. The bond angles of the vanadyl moiety, 109.81(11)° in molecule A and 109.50(9)° in molecule B, lie within the range 107−111° reported for a broad spectrum of dioxovanadium(V) complexes.[101,102,104,105,112−117,123] Generally, when the vanadyl oxygen atoms are not engaged in H-bonding interactions, the V═O distances range from 1.60 to 1.64 Å, with subtle differences between them, the one in the basal plane being somewhat longer presumably on account of a modest *trans* influence. This structural feature is observed in the independent molecules of complex **3** (Figure 4, Table 3). When either of the vanadyl oxygen atoms participates in H-bonding, its bonding to the vanadium(V) center is somewhat weakened, thereby causing significant lengthening of the V═O bond (∼1.66−1.69 Å).[114,126]

EPR Spectroscopy of Copper(II) Complexes. As already established by magnetic susceptibility measurements, the ternary complexes [Cu(Dpk-H-44mT)(phen)]$(ClO_4)_2$·1(1/2)MeOH (**1**·1(1/2)MeOH) and [Cu(Dpk44mT)(phen)]-ClO_4 (**2**) are paramagnetic with one unpaired electron. The X-band EPR spectrum of **1**·1(1/2)MeOH which was recorded in frozen MeOH solution at 77 K is shown in Figure 5. The spin Hamiltonian parameters g_z = 2.175, $g_{x,y}$ = 2.06, $A_z = 198 \times 10^{-4}$ cm^{-1} and $A_{x,y} \sim 10 \times 10^{-4}$ cm^{-1} from the simulated axial spectrum are indicative of a $d_{x^2-y^2}$ ground state ($g_z > g_{x,y} > 2.00$; $A_z > A_{x,y}$)[76,122,127−129] implying that the crystallographically determined solid-state coordination geometry is retained in solution. The degree of the extent of the tetragonal distortion as revealed by the value of g_z/A_z (110 cm) is comparable with those of the closely related ternary complexes of copper(II) with 2-formylpyridine-4-phenyl-3-thiosemicarbazone and heterocyclic bidentate ligands.[76] The EPR spectra of polycrystalline samples of **1**·1(1/2)MeOH and **2** [Figure S4] gave the following approximate values of g_z and $g_{x,y}$: 2.17 and 2.05, respectively, for the former and 2.15 and 2.05, respectively, for the latter, consistent with the structural analyses.

Electronic Absorption Spectroscopy of the Complexes. The discernible differences in the colors of the copper(II) complexes (**1**·1(1/2)MeOH and **2**) especially in solution (olive and olive brown, respectively, as can be seen from Figure 6), point to subtle structural differences in their coordination spheres. They have an intense visible absorption at 433 nm (ε_{max} = 19,850 and 23,620 dm^3 mol^{-1} cm^{-1}, respectively) in common, which is assignable to an LMCT transition. The lopsidedness of this broad absorption band suggests an occurrence of an additional electronic transition; the shoulder around 412 nm [Figure 6a inset] probably arises from an intraligand transition akin to that reported for $[Zn(Dpk44mT)_2]$ (λ = 416 nm, $\varepsilon \sim$ 14,795 dm^3 mol^{-1} cm^{-1}),[122] a complex having a metal center with the 3d-subshell fully occupied. Another similarity in the visible spectra of **1**·1(1/2)MeOH and **2** is the occurrence of a d-d absorption band at ∼660 nm ($\varepsilon \sim$ 320 and 330 dm^3 mol^{-1} cm^{-1}, respectively).[76,127] Copper(II) centers in a distorted square-based pyramidal coordination geometry tend to exhibit broad ligand-field absorptions in the visible region, sometimes extending to the near-IR region, in electronic spectra which are attributable to $d_{xz,yz} \rightarrow d_{x^2-y^2}$ and $d_{xy} \rightarrow d_{x^2-y^2}$ transitions.[127] A noticeable difference is the absorption at ∼520 nm appearing as a shoulder in the electronic spectrum of complex **1**·1(1/2)MeOH, but missing from that of complex **2**, which might explain the color difference between these two copper(II) compounds [Figure 6b]. This visible absorption most likely arises from the protonation of the di(2-pyridyl) moiety of the ligand in **1**·1(1/2)MeOH. Given its relatively higher energy and higher molar absorptivity than those of d-d absorptions coupled with the similarity of the coordination geometries of complexes **1**·1(1/2)MeOH and **2** (which precludes a difference between their ligand-field transitions), this visible absorption probably originates from a CT transition.

The reddish orange crystals of $[VO_2(Dpk44mT)]$ (**3**) dissolve in MeOH to form a strong orange-yellow solution whose electronic absorption spectrum is displayed in Figure 6c along with that of the free ligand. The lowest-energy intense broad ultraviolet (UV) absorption band of HDpk44mT (λ = 335, ε_{max} = 10,800 dm^3 mol^{-1} cm^{-1}) whose tail extends into the higher-energy end of the visible spectrum imparts the pale greenish yellow color to this ligand in solution. The pertinent

https://doi.org/10.1021/acsomega.5c01984
ACS Omega 2025, 10, 23440−23460

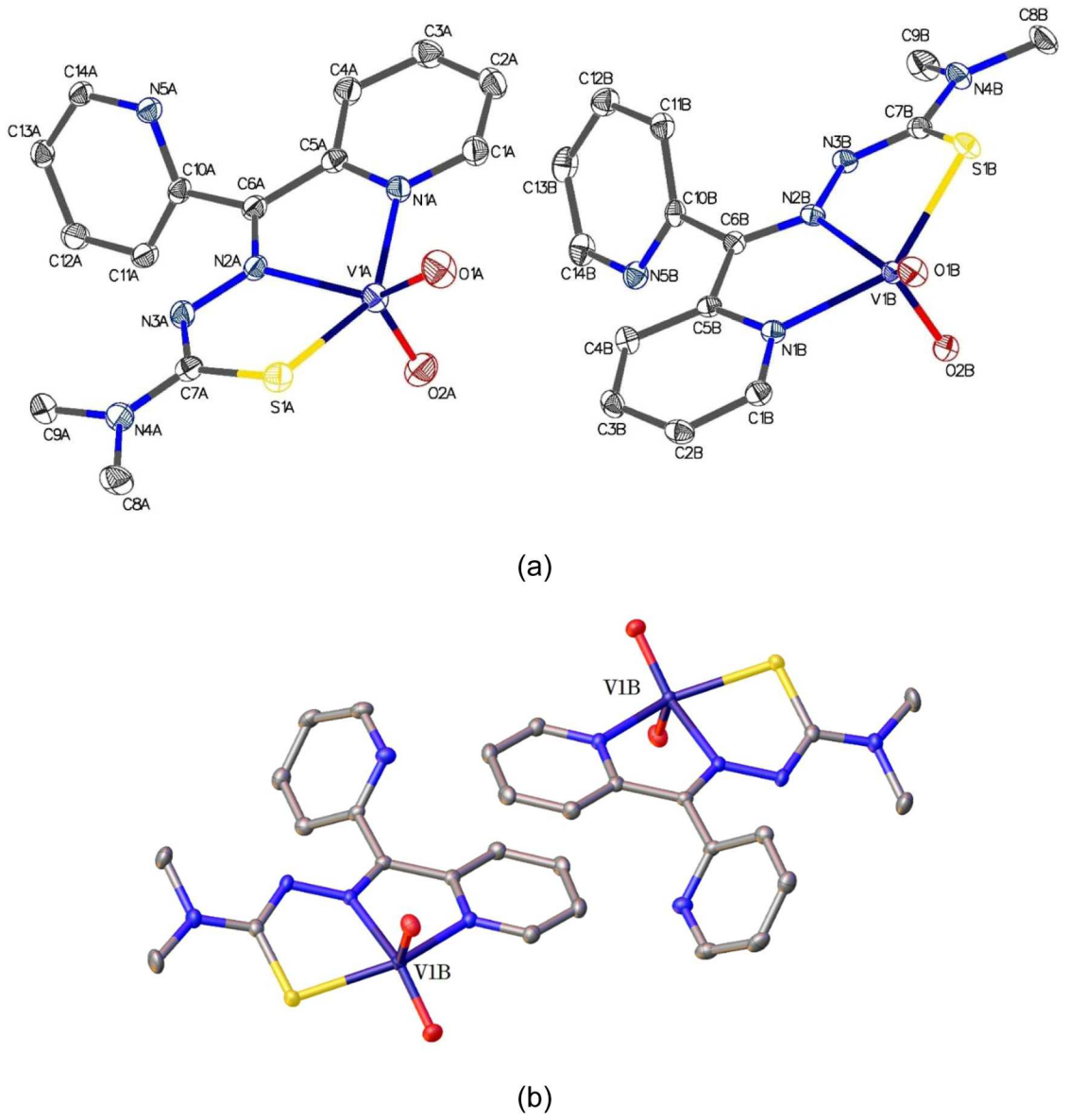

Figure 4. X-ray crystal structure of $[VO_2(Dpk44mT)]$ (**3**): (a) two independent molecules in the crystallographic asymmetric unit, (b) $\pi-\pi$ stacking interaction of molecules B.

electronic transition also occurs within the thio-enolate ligand which is coordinated to the $[VO_2]^+$ ion in complex **3** (λ = 330, ε_{max} = 12,000 dm^3 mol^{-1} cm^{-1}). The visible spectrum of **3** is dominated by the LMCT band at 458 nm (ε_{max} = 9,410 dm^3 mol^{-1} cm^{-1}).[102] As is always the case with dioxovanadium(V) complexes, ligand-field absorptions are nonexistent on account of the vacant d-subshell of the central metal ion.

NMR Spectroscopy of HDpk44mT and $[VO_2(Dpk44mT)]$. The thiosemicarbazone ligand HDpk44mT and its dioxovanadium(V) complex $[VO_2(Dpk44mT)]$ were characterized by ^{1}H- and ^{13}C NMR spectroscopic techniques and, additionally, in the case of the latter, by ^{51}V-NMR spectroscopy. We have elucidated the solution structures of these compounds largely from their ^{1}H NMR spectra which were recorded in DMSO-d_6 at a radiofrequency of 700 MHz. The chemical shifts, referenced to TMS as an internal standard (δ = 0), for the resonances in the ^{1}H NMR spectra were assigned in accordance with spin−spin splitting patterns, magnitudes of the coupling constants and ^{1}H−^{1}H COSY. Moreover, a comparison of the ^{1}H NMR spectrum of HDpk44mT with those of other members of the HDpkT series as well as those of thiosemicarbazones derived from 2-formylpyridine, 2-acetylpyridine and 2-benzoylpyridine is instructive. Similarly, the literature ^{1}H NMR spectra of the corresponding pyridyl and di(2-pyridyl) aroylhydrazones provide invaluable structural information in solution, particularly because of the greater propensity of their *E*/*Z*-isomers (Chart S1) to undergo interconversion in solution. A close and systematic inspection of the ^{1}H NMR spectra across a wide spectrum of pyridyl hydrazones has revealed a reliable distinguishing NMR trend between the *E*- and *Z*-isomers involving the chemical shifts of the resonances of the hydrazinic proton (i.e., = N−N*H*−C═X, X = O, S, Se) and the pyridyl α-proton (adjacent to the pyridyl nitrogen atom) (Chart S1).[7,15,20,34,36−38,42,48,53−63] For the *E*-isomer, the resonances of these two protons tend to occur in the ranges δ 10.15−11.50 and δ 8.57−8.64, respectively. In sharp contrast, for the *Z*-isomer, which exhibits intramolecular H-

https://doi.org/10.1021/acsomega.5c01984
ACS Omega 2025, 10, 23440−23460

Table 3. Selected Bond Distances (Å) and Angles (°) for [VO_2(Dpk44mT)] (3)

	molecule A	molecule B
V1−O1	1.633(2)	1.6405(17)
V1−O2	1.622(2)	1.6159(17)
V1−N1	2.098(2)	2.095(19)
V1−N2	2.142(2)	2.1653(19)
V1−S1	2.3652(8)	2.3676(7)
C7−S1	1.746(3)	1.759(2)
C6−N2	1.307(3)	1.308(3)
N2−N3	1.367(3)	1.365(3)
C7−N3	1.338(3)	1.331(3)
C7−N4	1.342(3)	1.343(3)
O1−V1−S1	97.25(8)	96.87(6)
O1−V1−N1	94.72(9)	95.93(8)
O1−V1−N2	142.74(10)	143.21(8)
O2−V1−S1	103.73(7)	105.10(7)
O2−V1−O1	109.81(11)	109.50(9)
O2−V1−N1	99.66(9)	99.81(8)
O2−V1−N2	107.16(9)	107.08(8)
N1−V1−S1	148.20(6)	146.20(6)
N1−V1−N2	74.56(8)	74.00(7)
N2−V1−S1	78.14(6)	77.05(5)

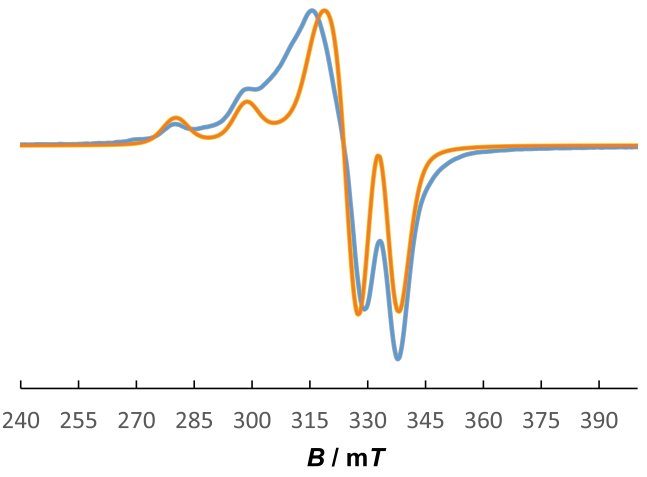

Figure 5. X-band EPR spectrum of [Cu(Dpk-H-44mT)(phen)]-$(ClO_4)_2$·1(1/2)MeOH (**1**·1(1/2)MeOH) in frozen methanol solution at 77 K (ν = 9.4 GHz): experimental (blue) and simulated (orange).

bonding between the hydrazinic proton and the pyridyl nitrogen, this pair of proton resonances appears consistently more downfield in the ranges δ 14.70−15.86 and δ 8.79−8.98, respectively.

The whole-range ^{1}H NMR spectra of HDpk44mT·H_2O and [VO_2(Dpk44mT)] (**3**) are presented in Figures S5 and S6, respectively. The spectrum of HDpk44mT shows the thioamide proton to be the most deshielded (δ 14.92), consistent with existence of this ligand in the *Z*-isomeric form as demonstrated crystallographically (Figure 1 and Chart 1). Consequently, the two pyridyl moieties of HDpk44mT are spectroscopically nonequivalent; indeed, as can be seen from Figure 7a, the spectrum shows the pyridyl proton peaks in duplicate. Consistently, for each pyridyl ring, the α-proton (H^A/H^a) is the most deshielded whereas the β-proton (H^B/

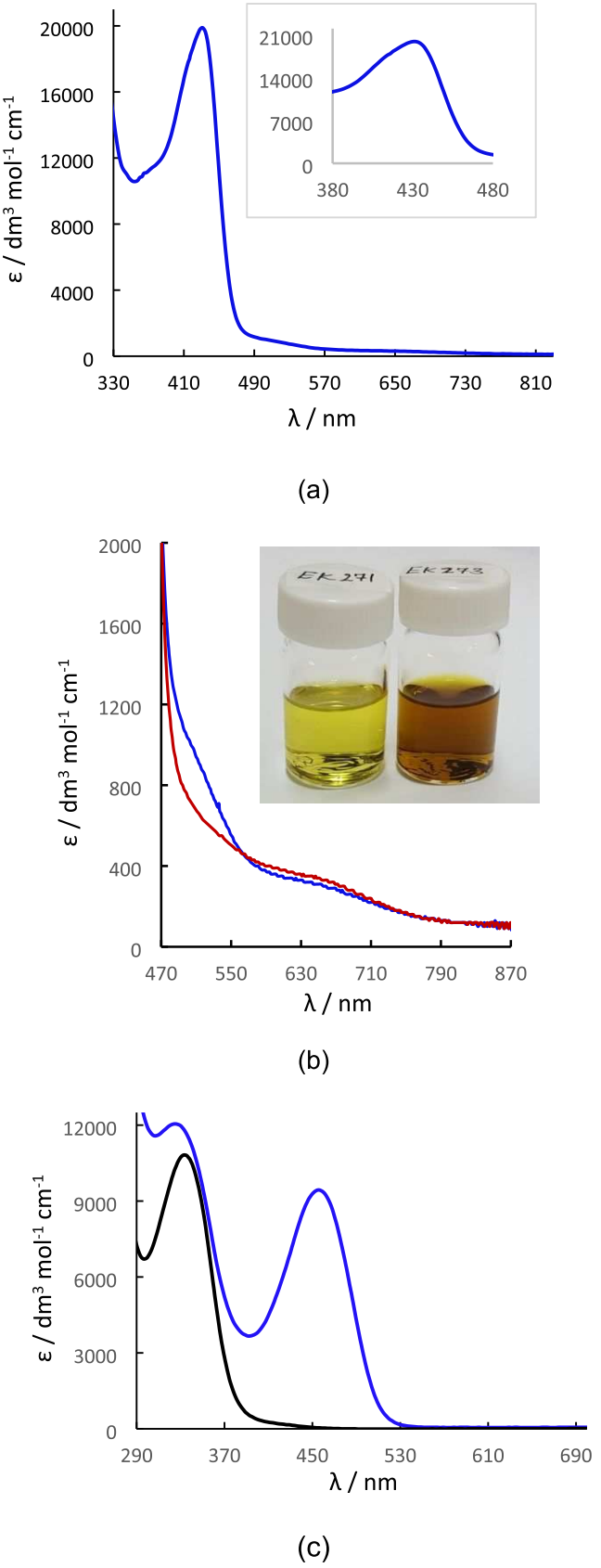

Figure 6. UV−visible spectra of (a) **1**·1(1/2)MeOH, (b) **1**·1(1/2)MeOH (blue line, olive solution) and **2** (red line, olive-brown solution), and (c) HDpk44mT (black line) and **3** (blue line) in MeOH.

https://doi.org/10.1021/acsomega.5c01984
ACS Omega 2025, 10, 23440−23460

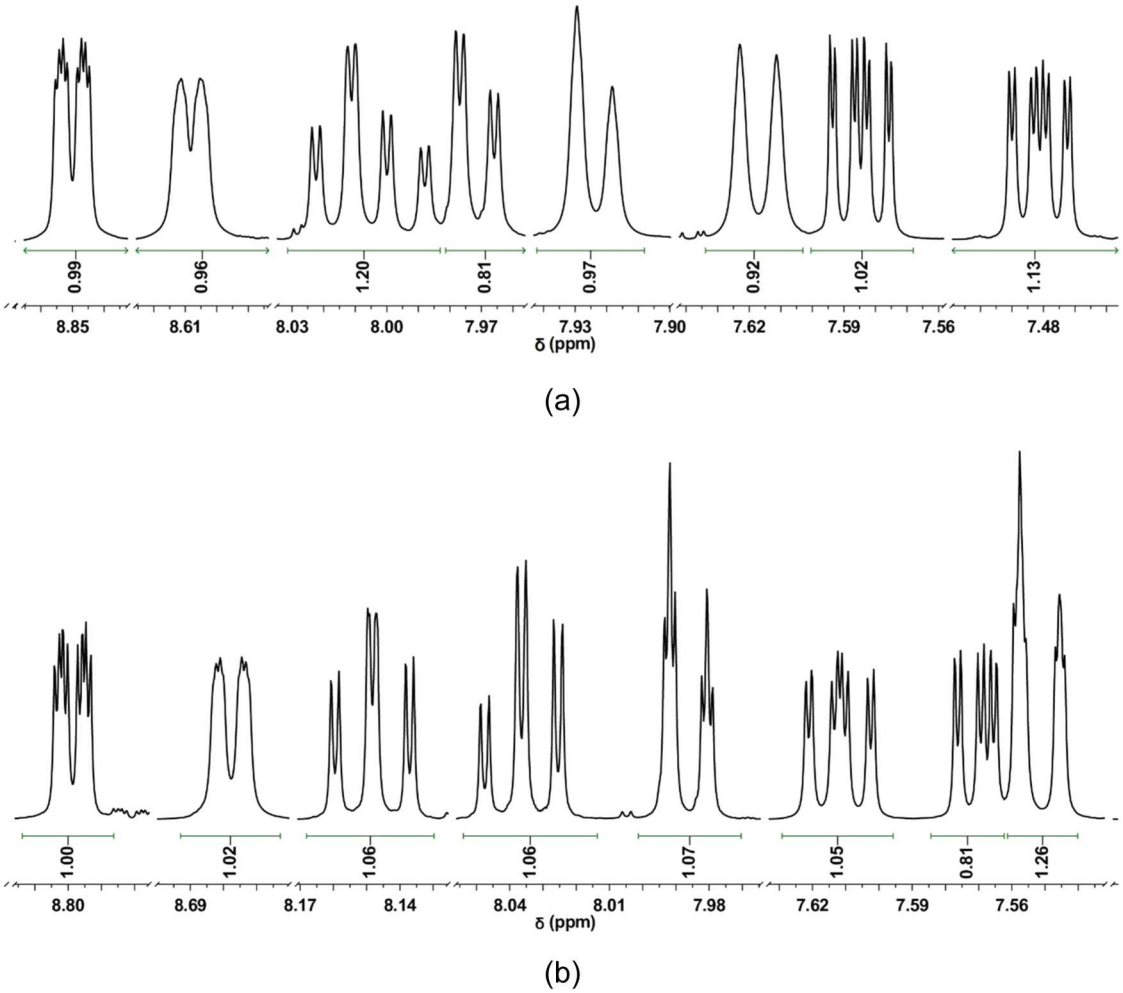

Figure 7. Aromatic regions of ^{1}H NMR spectra of (a) HDpk44mT·H_2O and (b) $[VO_2(Dpk44mT)]$ (**3**).

H^b) is the most shielded. Of the two α-protons, H^A (of the H-bonded pyridyl moiety) occurs more downfield at δ 8.85 (*cf.* δ 8.61 for H^a). The spectroscopic data and peak assignments are compiled in Table 4. The ^{1}H NMR spectrum of the complex $[VO_2(Dpk44mT)]$ is displayed in Figure 7b. The two pyridyl moieties have been rendered spectroscopically nonequivalent by the coordination of the nitrogen donor atom of one of them to the vanadium(V) ion, giving rise to the occurrence of twin peaks for the pyridyl proton resonances, the α-proton of the metal-bound pyridyl ring being more deshielded than that of the metal-free ring (δ 8.80 for H^A *vs* δ 8.68 for H^a). Two conspicuous differences between the ^{1}H NMR spectra of the ligand and the dioxovanadium(V) complex are as follows: (1) the doublet-of-triplet (dt) resonances are well-resolved in the latter whereas they are unresolved in the former, and (2) the dt resonance for H^d (of the metal-free pyridyl ring) in the complex appears surprisingly more upfield than that of the β-proton (H^b). The explanation for this behavior is complicated by the fact that the upfield shift occurs on the free pyridyl ring. In a previous study based on 2-acetylpyridine thiosemicarbazones, this phenomenon involved the corresponding proton of the pyridyl ring bound to the metal center and so this upfield shift was attributed to the coordination of the azomethine nitrogen.[104]

In the ^{13}C NMR spectrum of HDpk44mT the resonance at δ180.50 is attributable to the thione carbon, which for closely related thiosemicarbazones is observed in the range δ177–181.[20,34,36−38,104,105] The concomitant tautomeric transformation of this ligand and its complexation with the vanadium(V) ion in $[VO_2(Dpk44mT)]$ is evidenced by the new signal at δ177.42 ascribable to the thio-enolate carbon. The few known crystallographically *and* spectroscopically characterized dioxovanadium(V) complexes with pyridyl-based thiosemicarbazones exhibit similar behavior with $\Delta\delta_C$ ranging from −3 to −7 [$\Delta\delta_C = \delta_C(\text{complex}) - \delta_C(\text{ligand})$].[104] Coordination of the imine nitrogen of HDpk44mT to the vanadium(V) atom causes an enormous increase in the chemical shift of the associated carbon atom from δ156.28 to 207.00, indicative of considerable deshielding, as observed for closely related dioxovanadium(V) complexes.[114,116,130]

The ^{51}V-NMR spectrum of $[VO_2(Dpk44mT)]$ (Figure 8), recorded in DMSO-d_6 at 105 MHz with $VOCl_3$ as the reference standard (δ = 0), exhibits a strong resonance at δ −428, a chemical shift that compares favorably with those reported for similar dioxovanadium(V) complexes with *pyridyl*-based thiosemicarbazones and thiosemicarbazates possessing the $[N_{pyridyl}N_{imine}S_{thioenolate}]$ donor set which range from δ −415 to −444.[102,105,116,124] In contrast, the ^{51}V NMR signal for *phenolate*-based thiosemicarbazone or thiosemicarbazate complexes with dioxovanadium(V) is observed relatively more upfield typically between δ −465 and −473.[114,130] Evidently, the $\delta(^{51}$V-NMR) resonance for the $[VO_2]^+$ moiety is sensitive

https://doi.org/10.1021/acsomega.5c01984
ACS Omega 2025, 10, 23440−23460

Table 4. ^{1}H NMR Spectroscopic Data[a] for HDpk44mT·H_2O and $[VO_2(Dpk44mT)]$ (3)

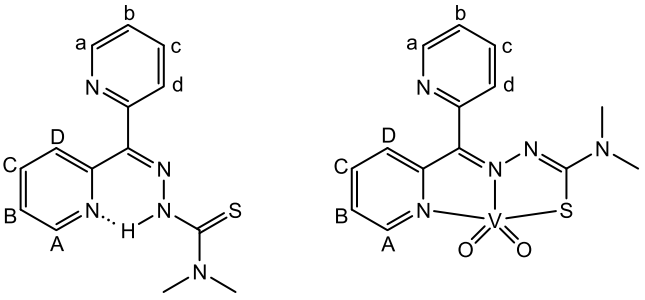

protons	HDpk44mT	$[VO_2(Dpk44mT)]$
−NH−	14.92 (s)	
$-N(CH_3)_2$	3.34(s)	3.33(s)
	hydrogen-bonded py	*vanadium-coordinated py*
H^A	8.85 (ddd, *J* = 4.9, 1.7, 0.9 Hz)	8.80 (ddd, *J* = 4.8, 1.7, 1.0 Hz)
H^B	7.58 (ddd, *J* = 7.6, 4.9, 1.1 Hz)	7.57 (ddd, *J* = 7.6, 4.9, 1.3 Hz)
H^C	8.01 (ddd, *J* = 7.8, 7.9, 1.8 Hz)	8.04 (ddd, *J* = 7.7, 7.7, 1.8 Hz)
H^D	7.62 (dt, unresolved, *J* = 8.1 Hz)	7.99 (dt, *J* = 7.8, 1.1 Hz)
	Free py	*Free py*
H^a	8.61 (ddd, unresolved)	8.68 (ddd, partially resolved, *J* = 5.4, 0.8 Hz)
H^b	7.48 (ddd, *J* = 7.5, 4.8, 1.2 Hz)	7.61 (ddd, *J* = 7.6, 5.5, 1.3 Hz)
H^c	7.98 (ddd, *J* = 7.70, 7.70, 1.75 Hz)	8.15 (ddd, *J* = 7.9, 7.9, 1.6 Hz)
H^d	7.92 (dt, unresolved, *J* = 7.8 Hz)	7.55 (dt, *J* = 8.4, 1.0 Hz)

[a]Assignments confirmed with 2-D NMR experiments.

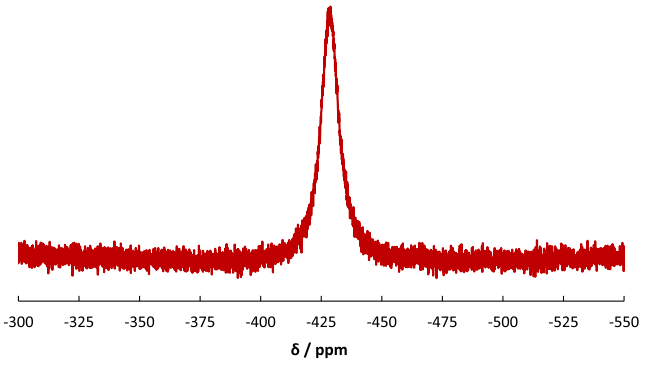

Figure 8. ^{51}V-NMR spectrum of $[VO_2(Dpk44mT)]$ (3) in DMSO-d_6 at 105 MHz.

to the coordination environment; replacement of the thioenolate sulfur atom with an oxygen (*e.g.*, enolate,[131−133] alkoxo,[134] or carboxylate[135]) or a nitrogen (*e.g.*, amine[136] or benzimidazole[137,138]) donor atom causes even greater shielding with chemical shifts between δ −500 and −570.

Pharmacological Properties and Redox Chemistry. The antiproliferative activity of complexes **1**·1(1/2)MeOH, **2** and **3** was investigated in two cancer cell lines, namely human cervical carcinoma (HeLa) and human breast adenocarcinoma (MCF-7), along with the normal (noncancerous) human breast epithelial cell line (MCF-10A), using the MTT cell viability assay [MTT = 3-(4,5-dimethylthiazol-2-yl)-2,5-diphenyltetrazolium bromide] which entails cleavage of the tetrazolium rings of MTT by mitochondrial dehydrogenases of viable cells resulting in the formation of dark purple membrane-impermeable crystals of formazan quantifiable in DMSO solution by visible spectroscopy. Although HDpk44mT is a well-established anticancer agent, the purpose of including it in the cytotoxicity evaluation was to allow a direct comparison of its potency with those of its new complexes (**1**·1(1/2)MeOH, **2** and **3**) under the same experimental conditions. The values of the 50% inhibitory concentrations (IC_{50}) of these substances together with the positive controls (docetaxel and paclitaxel) were determined as exemplified for complexes **1**·1(1/2)MeOH and **3** in the HeLa cells (Figure 9).

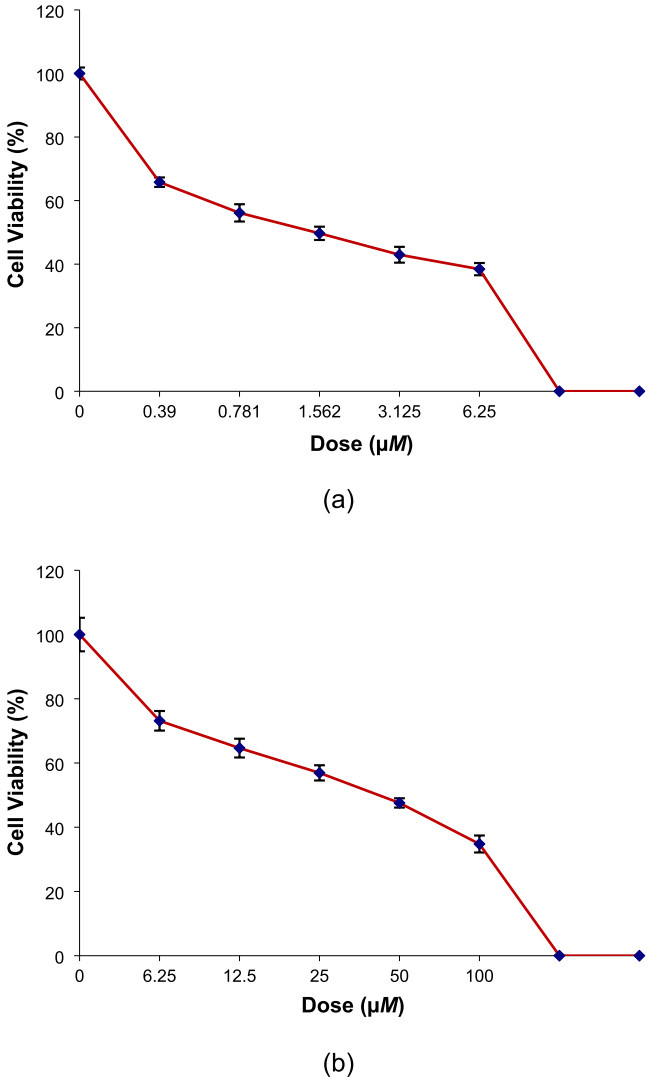

Figure 9. Cytotoxicity curves for (a) [Cu(Dpk-H-44mT)(phen)]-$(ClO_4)_2$·1(1/2)MeOH (**1**·1(1/2)MeOH) and (b) $[VO_2(Dpk44mT)]$ (**3**) in the HeLa cell line obtained after a 48-h incubation period.

The antiproliferative potential of each substance was tested within the 0.01−100-μM range of concentrations; the results of these cytotoxicity measurements are presented in Table 5. IC_{50} values for cisplatin (against HeLa,[139] MCF-7[140] and MCF-10A[141]), phen (against MCF-7[90]) and $Cu(ClO_4)_2·6H_2O$ (against MCF-7[90]) were obtained from the literature for the purpose of comparison.

https://doi.org/10.1021/acsomega.5c01984
ACS Omega 2025, 10, 23440−23460

Table 5. Cytotoxicity Evaluation of Compounds by MTT Assay in Cancer and Normal Cell Lines

compound	IC_{50} values/μM (after 48-h incubation period)		
	HeLa	MCF-7	MCF-10A
HDpk44mT	2.23 ± 0.28	0.58 ± 0.02	25.13 ± 2.06
[Cu(Dpk-H-44mT)(phen)]$(ClO_4)_2$·1(1/2)MeOH	1.64 ± 0.23	0.50 ± 0.03	0.47 ± 0.09
[Cu(Dpk44mT)(phen)]ClO_4	5.22 ± 0.61	0.36 ± 0.09	0.67 ± 0.11
[VO_2(Dpk44mT)]	42.93 ± 3.17	0.89 ± 0.07	19.22 ± 2.25
docetaxel	60.70 ± 5.13	92.54 ± 7.99	>100
paclitaxel	15.84 ± 1.28	>100	>100
cisplatin	13.28 ± 3.84[139]	13.36 ± 1.25[140]	91 ± 7[141]
phen		6.1 ± 0.5[90]	
$Cu(ClO_4)_2$·$6H_2O$		6.4 ± 0.5[90]	

Characteristic of its anticancer behavior, HDpk44mT selectively inhibited proliferation of the HeLa and MCF-7 cancer cells over the MCF-10A normal cells. However, its copper(II) complexes **1**·1(1/2)MeOH and **2** were indiscriminately potent against all three cell lines. It is noteworthy that the ligand and complexes **1**·1(1/2)MeOH and **2** exhibited comparable cytotoxicity toward the cancer cells, with slightly higher antiproliferative efficacy toward the MCF-7 cancer cells. Complexes **1**·1(1/2)MeOH and **2** are cytotoxic toward the HeLa cancer cells to a somewhat comparable extent to that reported for the similar complex [Cu(L)(phen)]ClO_4 (HL = 2-formylpyridine 4-phenyl-3-thiosemicarbazone).[76] Although **1**·1(1/2)MeOH and **2** have greater cytotoxicity potency than cisplatin against the HeLa and MCF-7 cancer cells, their lack of selectivity over MCF-10A renders them unsuitable as *in vivo* drugs. In contrast, the dioxovanadium(V) complex (**3**) bears the hallmarks of a promising drug in cancer treatment. It is ∼50-fold more cytotoxic toward MCF-7 than HeLa and its selectivity factor over MCF-10A [SF = IC_{50}(MCF-10A)/IC_{50}(MFC-7)] exceeds 20. In contrast, cisplatin is equally potent toward these two cancer cells judging by the reported comparable IC_{50} values (Table 5).[139,140] Thus, *in vitro*, complex **3** appears to be a better antiproliferative agent than cisplatin for targeted cancer treatment. Additionally, complex **3** exhibits higher antiproliferative efficacy toward MCF-7 than does the closely related dioxovanadium(V) complex of acetylpyridine 4-(*p*-fluorophenyl)-3-thiosemicarbazone (IC_{50} = 90.6 ± 0.97 μM, after a 48-h incubation period).[102] There exist a paucity of dioxovanadium(V) complexes with pyridyl-based thiosemicarbazones which have been investigated for anticancer activity.[105]

Invariably, copper(II) thiosemicarbazone complexes are redox-active,[8,16,18,20,76,122] the redox couple $Cu^{II/I}$ being the most prevalent. The electrochemical properties of complexes **1**·1(1/2)MeOH, **2** and **3** were investigated by cyclic voltammetry using a three-electrode electrochemical cell comprising a glassy carbon working electrode, an Ag/AgCl reference electrode and a Pt wire auxiliary electrode (NB: $E_{Ag/AgCl}$ + 197 mV = E_{NHE}; $E_{Ag/AgCl}$ − 45 mV = E_{SCE}; E_{SCE} + 242 mV = E_{NHE}; $E_{Ag/AgCl}$ − 444 mV = E_{Fc/Fc^+}; E_{Fc/Fc^+} + 640 mV = E_{NHE}). The cyclic voltammograms were recorded at a scan rate of 100 mV/s within the potential window −2.5 to +1.5 V in dry CH_2Cl_2 and MeOH (∼1 mM solutions of the complexes) under argon with 0.1 *M* [*n*-Bu_4N]PF_6 as the supporting electrolyte. Although the solubility of the complexes was slightly lower in MeOH than in CH_2Cl_2, solutions of the complexes [Cu(Dpk-H-44mT)(phen)]$(ClO_4)_2$·1(1/2)MeOH (**1**·1(1/2)MeOH) and [VO_2(Dpk44mT)] (**3**) in the former solvent afforded better defined cyclic voltammograms (Figure S7). On the other hand, solutions of [Cu(Dpk44mT)(phen)]ClO_4 (**2**) in both solvents gave well-defined cyclic voltammograms (Figure 10). The copper(II) complexes **1**·1(1/2)MeOH and **2** exhibit a reversible one-electron reduction associated with the Cu(II)/Cu(I) redox couple having half-wave redox potentials of −0.28 V (ΔE_p = 130 mV) *vs* Fc/Fc^+ ($E_{1/2}$ = +0.36 V *vs* NHE) and −0.96 V (ΔE_p = 280 mV) *vs* Fc/Fc^+ ($E_{1/2}$ = −0.32 V *vs* NHE),

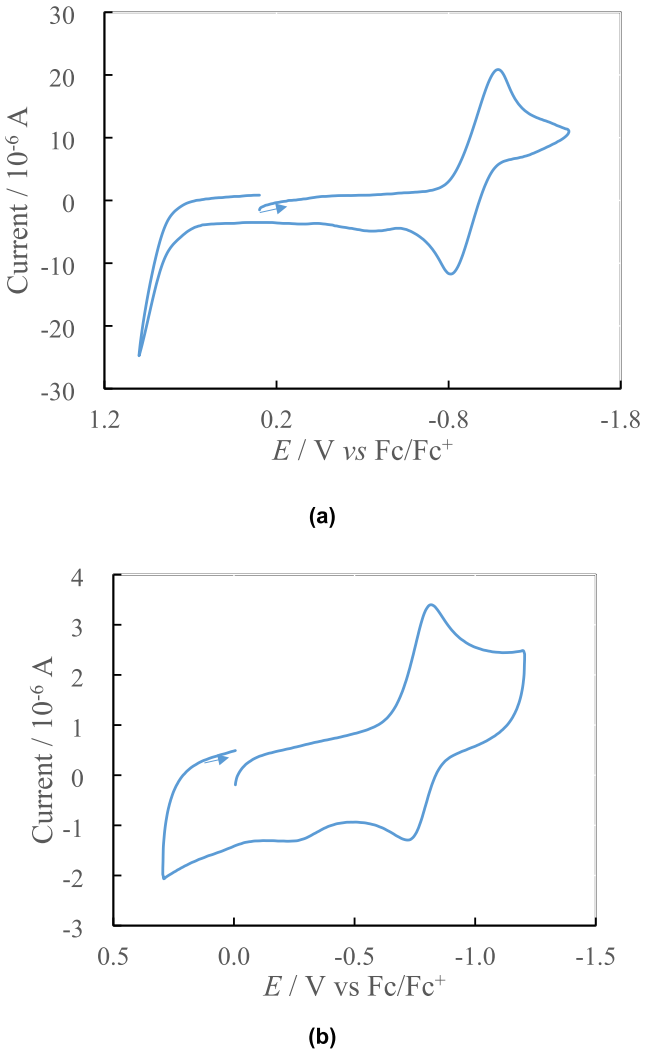

Figure 10. Cyclic voltammograms for [Cu(Dpk44mT)(phen)]ClO_4 (**2**) in (a) CH_2Cl_2 and (b) MeOH (∼1 mM solutions) and 0.1 M [*n*-Bu_4N]PF_6 supporting electrolyte (scan rate = 100 mV/s).

https://doi.org/10.1021/acsomega.5c01984
ACS Omega 2025, 10, 23440−23460

respectively, in CH_2Cl_2. The corresponding half-wave redox potentials for these complexes in MeOH are −0.38 V (ΔE_p = 100 mV) *vs* Fc/Fc^+ ($E_{1/2}$ = +0.26 V *vs* NHE) and −0.78 V (ΔE_p = 90 mV) *vs* Fc/Fc^+ ($E_{1/2}$ = −0.14 V *vs* NHE), respectively.

The trend in this CV experiment is that the reduction of the central metal ion occurs more spontaneously in complex **1**·1(1/2)MeOH than in complex **2** as evidenced by the anodic shift presumably due to the protonation of the thiosemicarbazonate ligand in the former. More importantly, the values of the reduction potentials lie within the biologically accessible redox potential window,[67] and are capable of inducing intracellular generation of reactive oxygen species (ROS) leading to cytotoxicity and cell death. The electrochemical properties of these copper(II) complexes are comparable with those of the closely related copper(II) ternary complexes of 2-formylpyridine 4-phenyl-3-thiosemicarbazone with bipy/phen or methyl-substituted derivative of bipy/phen as a coligand[76] as well as the binary complexes $[Cu(Dpk44mT)_2]$[122] and $[Cu(Ap44mT)_2]$,[16] all of which are highly antiproliferative against cancer cells. Finally, the cyclic voltammogram of $[VO_2(Dpk44mT)]$ (**3**) in MeOH [Figure S7(b)] shows four prominent cathodic potential (E_{pc}) peaks at −1.0, −1.3, −1.6 and −1.9 V, tentatively attributable to irreversible vanadium- and ligand-based reductions. The highest of these potentials is biologically relevant.[67]

CONCLUSIONS

Considering that HDpk44mT has drawn much attention over the years and has featured prominently in previous anticancer investigations, it is rather surprising that its X-ray structure has not been determined up until this research endeavor. Crystallographic analysis has demonstrated that it is isolated as the thioamide tautomer adopting the *Z*-configuration. Moreover, it has revealed that as a monohydrate, *i.e.*, $HDpk44mT{\cdot}H_2O$, the molecules of this thiosemicarbazone in the crystal lattice pack as 1D chains with intervening water molecules through H-bonding interactions. These chains are reinforced by π-π stacking interactions. NMR spectroscopy has shown that the tautomeric form and configuration of the free ligand remain intact in solution.

Reactions of equimolar amounts of $HDpk44mT{\cdot}H_2O$, $Cu(ClO_4)_2{\cdot}6H_2O$ and phen in refluxing MeOH produced the ternary ionic complexes $[Cu(Dpk\text{-}H\text{-}44mT)(phen)](ClO_4)_2{\cdot}1(1/2)MeOH$ (**1**·1(1/2)MeOH) and $[Cu(Dpk44mT)(phen)]ClO_4$ (**2**) under slightly acidic and moderately basic conditions, respectively. Treatment of **1**·1(1/2)MeOH with Et_3N in MeOH afforded **2**·MeOH. Thus, complex **2** was produced in both solvated and nonsolvated forms. Complexes **1**·1(1/2)MeOH and **2** are the first such ternary complexes of copper(II) with a *di(2-pyridyl)*-based thiosemicarbazone whose 3-D structures have been crystallographically determined. During the synthesis of each of these complexes, the thio-keto tautomer converted to the thio-enol tautomer concomitantly with deprotonation to bring about charge-neutrality upon complexation with the copper(II) ion. X-ray analyses of **1**·1(1/2)MeOH and **2** show the thiosemicarbazonate ligand coordinating meridionally while the bidentate phen coligand is nearly orthogonally oriented toward it. The resultant distorted square-pyramidal geometry at the metal center is subject to the Jahn−Teller effect as evidenced by the asymmetric coordination of phen with the axial $Cu{-}N_{phen}$ bond considerably elongated. EPR spectroscopic measurements of polycrystalline and frozen MeOH solution samples gave axial spectra consistent with a $d_{x^2-y^2}$ ground state. Electronic absorption spectroscopy detected subtle differences in the visible spectra of **1**·1(1/2)MeOH and **2** possibly responsible for the noticeable color differences. Both copper(II) complexes are highly cytotoxic toward the Hela and MCF-7 cell lines, but lack selectivity over normal MCF-10A cells. Both copper(II) ternary complexes are redox-active with the values of the potentials for the Cu(II)/Cu(I) redox couple lying within the biologically accessible redox potential window. Evidently, the anodic shift of the potentials of the zwitterionic complex (**1**·1(1/2)MeOH) points to greater spontaneity of the reduction process in this complex than in the deprotonated complex (**2**).

Intriguingly, attempts to synthesize the oxovanadium(IV) analog of the ternary copper(II) complexes (**1**·1(1/2)MeOH and **2**) by reacting $[VO(acac)_2]$ with $HDpk44mT{\cdot}H_2O$ in the presence of ClO_4^- as a possible counterion, afforded the complex $[VO_2(Dpk44mT)]$ (**3**) instead, which to the best of our knowledge, is the second such dioxovanadium(V) complex with a *di(2-pyridyl)*-possessing thiosemicarbazone crystallographically characterized. Complex **3** exhibits a severely distorted square-pyramidal coordination geometry with the oxo donors in axial−equatorial positions. The chemical shift of the broad ^{51}V-NMR signal reflects the nature of the donor environment. The electrochemistry of $[VO_2(Dpk44mT)]$ is complicated, but irreversible reduction processes have been revealed by the cyclic voltammogram of this complex in MeOH. Finally, the cytotoxicity evaluation of $[VO_2(Dpk44mT)]$ using the MTT cell viability assay has demonstrated that *in vitro* this complex is not only cancer-specific, but it is also selectively antiproliferative toward MCF-7 over MCF-10A. This *in vitro* anticancer activity makes this dioxovanadium(V) complex a promising candidate for further investigations including photocytotoxicity for photodynamic behavior, DNA binding/cleavage, ROS generation and apoptosis induction.

EXPERIMENTAL SECTION

Materials and Physical Techniques. All pertinent chemicals, reagents and solvents (HPLC/AR-grade) were purchased from Sigma-Aldrich save for vanadium(V) oxide and acetylacetone which were procured from BDH Chemicals LTD and Fluka Chemika, respectively, and used as received. Considering the notoriety of perchlorate salts for their tendency to explode, $Cu(ClO_4)_2{\cdot}6H_2O$ was used in minute quantities and handled with the utmost care. The ligand di(2-pyridyl) ketone 4,4-dimethyl-3-thiosemicarbazone (HDpk44mT) was synthesized and isolated as described in a literature procedure[13] with minor modifications. $[VO(acac)_2]$ was produced from the redox reaction between V_2O_5 and EtOH in the presence of Hacac with an adaptation of the well-known reported method,[142] and recrystallized from $CHCl_3$. Detailed synthetic procedures for the copper(II) and dioxovanadium(V) complexes are provided in the Supporting Information.

Microanalyses (CHN) were performed on a EuroEA or EuroVector elemental analyzer. Electrical conductivities of the complexes were determined with a JENWAY 4520 conductivity meter at room temperature using freshly prepared solutions (1 mM) in MeOH. FT-IR spectra were recorded on a PerkinElmer spectrophotometer (4000−400 cm^{-1}) with the samples compressed as KBr discs using a Specac press. ^1H- and

https://doi.org/10.1021/acsomega.5c01984
ACS Omega 2025, 10, 23440−23460

^{13}C NMR spectroscopic measurements were carried out at room temperature in DMSO-d_6 on a Bruker ASCEN 700 spectrometer operating at radiofrequencies of 700 and 176 MHz, respectively; the chemical shifts are referenced to TMS as an internal standard (δ = 0). The ^{51}V NMR spectrum of [VO_2(Dpk44mT)] was run at room temperature on a JNM-ECS400 spectrometer operating at a radiofrequency of 105 MHz, using $VOCl_3$ as an external reference standard (δ = 0). X-band EPR spectra of the copper(II) complexes were recorded on a Bruker ELEXSYS E580X FT CW spectrometer ($\nu \sim 9.4$ GHz) and a Bruker EMX Micro X spectrometer ($\nu \sim 9.6$ GHz). Electronic absorption spectra were measured with a Shimadzu 2450 UV−visible spectrophotometer (190−1000 nm) using freshly prepared solutions. Magnetic susceptibility measurements were carried out at room temperature using a Sherwood Scientific magnetic susceptibility balance. The magnetic data were corrected for diamagnetism using Pascal's constants the usual way ($x_{para} = x_{meas} - x_{dia}$). Cyclic voltammetry experiments were performed on a BAS 100BW Electrochemical Analyzer under a dry inert atmosphere at room temperature with potentials recorded between +1.5 and −2.5 V employing a conventional three-electrode cell comprising a glassy carbon disk (1.5 mm radius), platinum wire and Ag/Ag^+ ([n-Bu_4N]ClO_4/CH_3CN) as working, counter and reference electrodes, respectively. Cyclic voltammograms were measured in CH_2Cl_2 and MeOH ($\sim 10^{-3}$ M solutions of complexes) with 0.1 M [n-Bu_4N]PF_6 as the supporting electrolyte. All cyclic voltammograms were internally referenced to the Fc+/Fc redox couple.

Single-crystal X-ray structure determinations were carried out at low temperature (T = 100 or 110 K) on a Bruker APEX-II CCD area-detector diffractometer (Mo−Kα radiation, λ = 0.71073 Å) or on a XtaLAB Synergy R, HyPix-Arc 100 diffractometer (Cu−Kα radiation, λ = 1.54184 Å). The crystals were mounted in fomblin oil and cooled in a stream of cold N_2. Data were corrected for absorption using empirical methods (SADABS)[143] based upon symmetry equivalent reflections combined with measurements at different azimuthal angles.[144] The crystal structures were solved and refined against F^2 values using ShelXT[145] for solution and ShelXL[146] for refinement (using least-squares minimization) accessed *via* the Olex2 program.[147]

■ ASSOCIATED CONTENT

Supporting Information

The Supporting Information is available free of charge at https://pubs.acs.org/doi/10.1021/acsomega.5c01984.

Procedures for syntheses of compounds and anticancer investigation; chart of *E*/*Z*-isomers and conformations of pyridyl hydrazones; FT-IR spectra; ESI mass spectrum; X-ray packing diagram; EPR spectra; NMR spectra; cyclic voltammograms; selected crystallographic data; parameters for $\pi-\pi$ stacking interactions; H-bond data (PDF)

Accession Codes

CCDC 2416245, 2416246, 2416247, and 2416248 contain the supplementary crystallographic data for HDpk44mT·H_2O, **1**, **2** and **3**, respectively. These data can be obtained free of charge *via* www.ccdc,cam.ac.uk/data_request/cif or by e-mailing data_request@ccdc.cam.ac.uk, or by contacting The Cambridge Crystallographic Data Centre, 12 Union Road, Cambridge, CB2 1EZ, UK; fax: + 44 1223 336033.

■ AUTHOR INFORMATION

Corresponding Author

Musa S. Shongwe − *Department of Chemistry, College of Science, Sultan Qaboos University, 123 Muscat, Sultanate of Oman;* orcid.org/0000-0002-6382-3114; Email: musa@squ.edu.om

Authors

Iman K. Al Salmi − *Department of Chemistry, College of Science, Sultan Qaboos University, 123 Muscat, Sultanate of Oman;* Present Address: College of Engineering and Technology, University of Technology and Applied Sciences, PO Box 191, PC 314, Al Musannah, Sultanate of Oman

Hamad H. Al Mamari − *Department of Chemistry, College of Science, Sultan Qaboos University, 123 Muscat, Sultanate of Oman;* orcid.org/0000-0003-1684-2010

Craig C. Robertson − *School of Mathematical and Physical Sciences, University of Sheffield, Sheffield S3 7HF, UK*

Makoto Handa − *Department of Chemistry, Graduate School of Natural Science and Technology, Shimane University, Shimane 690-8504, Japan;* orcid.org/0000-0001-8943-2472

Shohreh Tavajohi − *Department of Toxicology and Pharmacology, Faculty of Pharmacy, Tehran University of Medical Sciences, Tehran 1417614411, Iran*

Adam Brookfield − *Department of Chemistry, The University of Manchester, Manchester M13 9PL, UK*

Eric J. L. McInnes − *Department of Chemistry, The University of Manchester, Manchester M13 9PL, UK;* orcid.org/0000-0002-4090-7040

Yoshihito Hayashi − *Department of Chemistry, Graduate School of Natural Science and Technology, Kanazawa University, Kakuma, Kanazawa 920-1192, Japan;* orcid.org/0000-0003-4896-9008

Ebrahim S. Moghadam − *Drug Design and Development Research Center, The Institute of Pharmaceutical Sciences (TIPS), Tehran University of Medical Sciences, Tehran 1417614411, Iran*

Complete contact information is available at: https://pubs.acs.org/10.1021/acsomega.5c01984

Notes

The authors declare no competing financial interest.

■ ACKNOWLEDGMENTS

Sultan Qaboos University is gratefully acknowledged for financial support (IKAl-S, PhD Bench Fees; MSS, Dean's Top-Up Grants: IG/SCI/DEAN/22/01 & IG/SCI/DEAN/23/01). We owe a debt of gratitude to the Central Analytical and Applied Research Unit (CAARU, College of Science, SQU) for the mass spectrometric and NMR spectroscopic measurements performed by Mr Sathish B. S. Pandian and Dr Samuel Premkumar, respectively. We also thank the EPSRC (U.K.) for funding of the EPR National Research Facility (EP/W014521/1, EP/X034623).

■ REFERENCES

(1) Lobana, T. S.; Sharma, R.; Bawa, G.; Khanna, S. Bonding and structure trends of thiosemicarbazone derivatives of metals − an overview. *Coord. Chem. Rev.* **2009**, *253*, 977−1055.

(2) Papathanasis, L.; Demertzis, M. A.; Yadav, P. N.; Kovala-Demertzi, D.; Prentjas, C.; Castiñeiras, A.; Skoulika, S.; West, D. X.

Palladium(II) and platinum(II) complexes of 2-hydroxyacetophenone *N*(4)-ethylthiosemicarbazone − crystal structure and description of bonding properties. *Inorg. Chim. Acta* **2004**, *357*, 4113−4120.
(3) Zhang, Z.; Gou, Y.; Wang, J.; Yang, K.; Qi, J.; Zhou, Z.; Liang, S.; Liang, H.; Yang, F. Four copper(II) compounds synthesized by anion regulation: structure, anticancer function and anticancer mechanism. *Eur. J. Med. Chem.* **2016**, *121*, 399−409.
(4) Lobana, T. S.; Kumari, P.; Butcher, R. J.; Jasinski, J. P.; Golen, J. A. Metal derivatives of thiosemicarbazones: crystal and molecular structures of mono- and dinuclear copper(II) complexes with N^1-substituted salicylaldehyde thiosemicarbazones. *Z. Anorg. Allg. Chem.* **2012**, *638*, 1861−1867.
(5) Lobana, T. S.; Kumari, P.; Castiñeiras, A.; Butcher, R. J. The effect of C-2 substituents of salicyladehyde-based thiosemicarbazones on the synthesis, spectroscopy, structures, and fluorescence of nickel(II) complexes. *Eur. J. Inorg. Chem.* **2013**, *2013*, 3557−3566.
(6) Kumari, P.; Lobana, S. T.; Butcher, R. J.; Castiñeiras, A.; Zeller, M. The effect of substituents at C^2/N^1 atoms of salicylaldehyde and 2-hydroxyacetophenone-based thiosemicarbazones on the nature of nickel(II) complexes with 1,10-phenanthroline and terpyridine as co-ligands. *Inorg. Chim. Acta* **2018**, *482*, 268−274.
(7) Pereiras-Gabián, G.; Vázquez-López, M.; Abram, U. Dimeric rhenium(I) carbonyl complexes with thiosemicarbazone backbone. *Z. Anorg. Allg. Chem.* **2004**, *630*, 1665−1670.
(8) (a) Qi, J.; Liang, S.; Gou, Y.; Zhang, Z.; Zhou, Z.; Yang, F.; Liang, H. Synthesis of four binuclear copper(II) complexes: structure, anticancer properties and anticancer mechanism. *Eur. J. Med. Chem.* **2015**, *96*, 360−368. (b) Qi, J.; Yao, Q.; Tian, L.; Wang, Y. Piperidylthiosemicarbazones Cu(II) complexes with a high anticancer activity by catalysing hydrogen peroxide to degrade DNA and promote apoptosis. *Eur. J. Med. Chem.* **2018**, *158*, 853−862.
(9) Al Salmi, I. K.; Shongwe, M. S. Ternary phenolate-based thiosemicarbazone complexes of copper(II): magnetostructural properties, spectroscopic features and marked selective antiproliferative activity against cancer cells. *Molecules* **2024**, *29*, No. 431.
(10) Duan, C.-Y.; Wu, B.-M.; Mak, T. C. W. Synthesis and structural characterization of new quadridentate N_3S-compound di-2-pyridyl ketone thiosemicarbazone and its binuclear copper(II) complexes. *J. Chem. Soc., Dalton Trans.* **1996**, 3485−3490.
(11) Lovejoy, D. B.; Richardson, D. R. Novel "hybrid" iron chelators derived from aroylhydrazones and thiosemicarbazones demonstrate selective antiproliferative activity against tumor cells. *Blood* **2002**, *100*, 666−676.
(12) Yuan, J.; Lovejoy, D. B.; Richardson, D. R. Novel di-pyridyl-derived iron chelators with marked and selective antitumor activity: in vitro and in vivo assessment. *Blood* **2004**, *104*, 1450−1458.
(13) Richardson, D. R.; Sharpe, P. C.; Lovejoy, D. B.; Senaratne, D.; Kalinowski, D. S.; Islam, M.; Bernhardt, P. V. Dipyridyl thiosemicarbazone chelators with potent and selective antitumor activity form iron complexes with redox activity. *J. Med. Chem.* **2006**, *49*, 6510−6521.
(14) Kalinowski, D. S.; Yu, Y.; Sharpe, P. C.; Islam, M.; Liao, Y.-T.; Lovejoy, D. B.; Kumar, N.; Bernhardt, P. V.; Richardson, D. R. Design, synthesis, and characterization of novel iron chelators: structure-activity relationships of the 2-benzoylpyridine thiosemicarbazone series and their 3-nitrobenzoyl analogues as potent antitumor agents. *J. Med. Chem.* **2007**, *50*, 3716−3729.
(15) Richardson, D. R.; Kalinowski, D. S.; Richardson, V.; Sharpe, P. C.; Lovejoy, D. B.; Islam, M.; Bernhardt, P. V. 2-Acetylpyridine thiosemicarbazones are potent iron chelators and antiproliferative agents: redox activity, iron complexation and characterization of their antitumor activity. *J. Med. Chem.* **2009**, *52*, 1459−1470.
(16) Jansson, P. J.; Sharpe, P. C.; Bernhardt, P. V.; Richardson, D. R. Novel thiosemicarbazones of the ApT and DpT series and their copper complexes: identification of pronounced redox activity and characterization of their antitumor activity. *J. Med. Chem.* **2010**, *53*, 5759−5769.
(17) Stefani, C.; Punnia-Moorthy, G.; Lovejoy, D. B.; Jansson, P. J.; Kalinowski, D. S.; Sharpe, P. C.; Bernhardt, P. V.; Richardson, D. R. Halogenated 2′-benzoylpyridine thiosemicarbazone (XBpT) chelators with potent and selective anti-neoplastic activity: relationship to intracellular redox activity. *J. Med. Chem.* **2011**, *54*, 6936−6948.
(18) Lovejoy, D. B.; Sharp, D. M.; Seebacher, N.; Obeidy, P.; Prichard, T.; Stefani, C.; Basha, M. T.; Sharpe, P. C.; Jansson, P. J.; Kalinowski, D. S.; Bernhardt, P. V.; Richardson, D. R. Novel second-generation di-2-pyridylketone thiosemicarbazones show synergism with standard chemotherapeutics and demonstrate potent activity against lung cancer xenografts after oral and intravenous administration in vivo. *J. Med. Chem.* **2012**, *55*, 7230−7244.
(19) Stefani, C.; Jansson, P. J.; Gutierrez, E.; Bernhardt, P. V.; Richardson, D. R.; Kalinowski, D. S. Alkyl substituted 2′-benzoylpyridine thiosemicarbazone chelators with potent and selective anti-neoplastic activity: novel ligands that limit methemoglobin formation. *J. Med. Chem.* **2013**, *56*, 357−370.
(20) Ohui, K.; Afanasenko, E.; Bacher, F.; Ting, R. L. X.; Zafar, A.; Blanco-Cabra, N.; Torrents, E.; Dömötör, O.; May, N. V.; Darvasiova, D.; Enyedy, E. A.; Popović-Bijelić, A.; Reynisson, J.; Rapta, P.; Babak, M. V.; Pastorin, G.; Arion, V. B. New water-soluble copper(II) complexes with morpholine-thiosemicarbazone hybrids: insights into the anticancer and antibacterial mode of action. *J. Med. Chem.* **2019**, *62*, 512−530.
(21) Wang, J.; Zhang, Z.-M.; Li, M.-X. Synthesis, characterization, and biological activity of cadmium(II) and antimony(III) complexes based on 2-acetylpyrazine thiosemicarbazones. *Inorg. Chim. Acta* **2022**, *530*, No. 120671.
(22) Savir, S.; Liew, J. W. K.; Vythilingam, I.; Lim, Y. A. L.; Tan, C. H.; Sim, K. S.; Lee, V. S.; Maah, M. J.; Tan, K. W. Nickel(II) complexes with polyhydroxybenzaldehyde and O,N,S tridentate thiosemicarbazone ligands: synthesis, cytotoxicity, antimalarial activity, and molecular docking studies. *J. Mol. Struct.* **2021**, *1242*, No. 130815.
(23) Rodríguez-Argüelles, M. C.; López-Silva, E. C.; Sanmartín, J.; Pelagatti, P.; Zani, F. Copper complexes of imidazole-2-, pyrrole-2- and indol-3-carbaldehyde thiosemicarbazones: inhibitory activity against fungi and bacteria. *J. Inorg. Biochem.* **2005**, *99*, 2231−2239.
(24) Genova, P.; Varadinova, T.; Matesanz, A. I.; Marinova, D.; Souza, P. Toxic effects of bis(thiosemicarbazone) compounds and its palladium(II) complexes on herpes simplex virus growth. *Toxicol. Appl. Pharmacol.* **2004**, *197*, 107−112.
(25) Karaküçük-İyidoğan, A.; Taşdemir, D.; Oruç-Emre, E. E.; Balzarini, J. Novel platinum(II) and palladium(II) complexes of thiosemicarbazones derived from 5-substitutedthiophene-2-carbaldehydes and their antiviral and cytotoxicity activities. *Eur. J. Med. Chem.* **2011**, *46*, 5616−5624.
(26) Bajaj, K.; Buchanan, R. M.; Grapperhaus, C. A. Antifungal activity of thiosemicarbazones, bis(thiosemicarbazones), and their metal complexes. *J. Inorg. Biochem.* **2021**, *225*, No. 111620.
(27) Khanye, S. D.; Smith, G. S.; Lategan, C.; Smith, P. J.; Gut, J.; Rosenthal, P. J.; Chibale, K. Synthesis and in vitro evaluation of gold(I) thiosemicarbazone complexes for antimalarial activity. *J. Inorg. Biochem.* **2010**, *104*, 1079−1083.
(28) Stacy, A. E.; Palanimuthu, D.; Bernhardt, P. V.; Kalinowski, D. S.; Jansson, P. J.; Richardson, D. R. Zinc(II)-thiosemicarbazone complexes are localized to the lysosomal compartment where they transmetallate with copper ions to induce cytotoxicity. *J. Med. Chem.* **2016**, *59*, 4965−4984.
(29) Stacy, A. E.; Palanimuthu, D.; Bernhardt, P. V.; Kalinowski, D. S.; Jansson, P. J.; Richardson, D. R. Structure-activity relationships of di-2-pyridylketone, 2-benzoyl, and 2-acetylpyridine thiosemicarbazones for overcoming Pgp-mediated drug resistance. *J. Med. Chem.* **2016**, *59*, 8601−8620.
(30) Krchniakova, M.; Paukovcekova, S.; Chlapek, P.; Neradil, J.; Skoda, J.; Veselska, R. Thiosemicarbazones and selected tyrosine kinase inhibitors synergize in pediatric solid tumors: NDRG1 upregulation and impaired prosurvival signalling in neuroblastoma cells. *Front. Phamacol.* **2022**, *13*, No. 976955.
(31) Shehadeh-Tout, F.; Milioli, H. H.; Roslan, S.; Jansson, P. J.; Dharmasivan, M.; Graham, D.; Anderson, R.; Wijesinghe, T.; Azad,

https://doi.org/10.1021/acsomega.5c01984
ACS Omega 2025, 10, 23440−23460

M. G.; Richardson, D. R.; Kovacevic, Z. Innovative thiosemicarbazones that induce multi-modal mechanisms to down-regulate estrogen-, progesterone-, androgen- and prolactin-receptors in breast cancer. *Pharmcol. Res.* **2023**, *193*, No. 106806.
(32) Ritacca, A. G.; Falcone, E.; Doumi, I.; Vileno, B.; Faller, P.; Sicilia, E. Dual role of glutathione as a reducing agent and Cu-ligand governs the ROS production by anticancer Cu-thiosemicarbazone complexes. *Inorg. Chem.* **2023**, *62*, 3957−3964.
(33) West, D. X.; Bain, G. A.; Butcher, R. J.; Jasinski, J. P.; Li, Y.; Pozdniakiv, R. Y.; Valdés-Martínez, J.; Toscano, R. A.; Hernández-Ortega, S. Structural studies of three isomeric forms of heterocyclic N(4)-substituted thiosemicarbazones and two nickel(II) complexes. *Polyhedron* **1996**, *15*, 665−674.
(34) Kowol, C. R.; Trondl, R.; Heffeter, P.; Arion, V. B.; Jacupec, M. A.; Roller, A.; Galanski, M. S.; Berger, W.; Keppler, B. K. Impact of metal coordination on cytotoxicity of 3-aminopyridine-2-carboxaldehyde thiosemicarbazone (Triapine) and novel insights into terminal demethylation. *J. Med. Chem.* **2009**, *52*, 5032−5043.
(35) Kumbhar, A.; Sonawane, P.; Padhye, S.; West, D. X.; Butcher, R. J. Structure of antitumor agents 2-acetylpyridinethiosemicarbazone hemihydrate and 2-acetylpyridinethiosemicarbazone hydrochloride. *J. Chem. Crystallogr.* **1991**, *27*, 533−539.
(36) Bermejo, E.; Castiñeiras, A.; Domínguez, R.; Carballo, R.; Maichle-Mössmer, C.; Strähle, J.; West, D. X. Preparation, structural characterization, and antifungal activities of complexes of Group 12 metals with 2-acetylpyridine- and acetylpyridine-N-oxide-^{4}*N*-phenylhiosemicarbazones. *Z. Anorg. Allg. Chem.* **1999**, *625*, 961−968.
(37) Bermejo, E.; Carballo, R.; Castiñeiras, A.; Domínguez, R.; Liberta, A. E.; Maichle-Mössmer, C.; Salberg, M. M.; West, D. X. Synthesis, structuralcharacteristics and biological activities of complexes of Zn^{II}, Cd^{II}, Hg^{II}, Pd^{II} and Pt^{II} with 2-acetylpyridine 4-mrthylthiosemicarbazone. *Eur. J. Inorg. Chem.* **1999**, *1999*, 965−973.
(38) Kowol, C. R.; Reisner, E.; Chiorescu, I.; Arion, V. B.; Galanski, M.; Deubel, D. V.; Keppler, B. K. An electrochemical study of antineoplastic gallium, iron and ruthenium complexes with redox noninnocent αN-heterocyclic chalcogensemicarbazones. *Inorg. Chem.* **2008**, *47*, 11032−11047.
(39) Casas, J. S.; Castellano, E. E.; Ellena, J.; Tasende, M. S. G.; Sánchez, A.; Sordo, J.; Vidarte, M. J. Compositional and structural varietyof diphenyllead(IV) complexes obtained by reaction of diphenyllead with thiosemicarbazones. *Inorg. Chem.* **2003**, *42*, 2584−2595.
(40) Lukmantara, A. Y.; Kalinowski, D. S.; Kumar, N.; Richardson, D. R. Synthesis and biological evaluation of substituted 2-benzoylpyridine thiosemicarbazones: novel structure-activity relationships underpinning their antiproliferative and chelation efficacy. *Bioorg. Med. Chem. Lett.* **2013**, *23*, 967−974.
(41) Muralisankar, M.; Haribabu, J.; Bhuvanesh, N. S. P.; Karvembu, R.; Sreekanth, A. Synthesis, X-ray crystal structure DNA/protein binding, DNA cleavage and cytotoxicity studies of N(4) substituted thiosemicarbazone based copper(II)/nickel(II) complexes. *Inorg. Chim. Ata* **2016**, *449*, 82−95.
(42) Swearingen, J. K.; West, D. X. Structural and spectral studies of di-2-pyridyl ketone *N*(4)-methyl- and *N*(4)-dimethylthiosemicarbazone and their metal complexes. *Transit. Met. Chem.* **2001**, *26*, 252−260.
(43) Almeida, C. M.; Nascimento, G. P.; Magalhães, K. G.; Iglesias, B. A.; Gatto, C. C. Crystal structures, DNA-binding ability and influence on cellular viability of gold(I) complexes of thiosemicarbazones. *J. Coord. Chem.* **2018**, *71*, 502−519.
(44) Suni, V.; Kurup, M. R. P.; Nethaji, M. Structural and spectral perspectives of a novel thiosemicarbazone synthesized from di-2-pyridyl ketone and 4-phenyl-3-thiosemicarbazide. *Spectrochim. Acta Part A* **2006**, *63*, 174−181.
(45) Usman, A.; Razak, I. A.; Chantrapromma, S.; Fun, H.-K.; Philip, V.; Sreekanth, A.; Kurup, M. R. P. Di-2-pyridyl ketone N^{4},N^{4}-(butane-1,4-diyl)thiosemicarbazone. *Acta Crystallogr.* **2002**, *C58*, o652−0654.
(46) Philip, V.; Suni, V.; Kurup, M. R. P. Di-2-pyridyl ketone 4-methyl-4-phenylthiosemicarbazone. *Acta Crystallogr.* **2004**, *60*, o856−o858.
(47) Conde, A.; López-Castro, A.; Márquez, R. The crystal and molecular structure of 2-formylpyridine selenosemicarbazone. *Acta Crystallogr.* **1972**, *28*, 3464−3469.
(48) Kowol, C. R.; Eichinger, R.; Jakupec, M. A.; galanski, M. S.; Arion, V. B.; Keppler, B. K. Effect of metal ion complexation and chalcogen donor identity on the antiproliferative activity of 2-acetylpyridine *N*,*N*-dimethyl(chalcogen)semicarbazones. *J. Inorg. Biochem.* **2007**, *101*, 1946−1957.
(49) Paschalidis, D. G.; Tossidis, I. A.; Gdaniec, M. Synthesis, characterization, and spectra of lanthanide(III) hydrazone complexes. The X-ray molecular structures of the erbium(III) complex and the ligand. *Polyhedron* **2000**, *19*, 2629−2637.
(50) Patole, J.; Sandbhor, U.; Padhye, S.; Deobagkar, D. N.; Anson, C. E.; Powell, A. Structural chemistry and in vitro antitubercular activity of acetylpyridine benzoyl hydrazone and its copper complex against *Mycobacterium smegmatis*. *Bioorg. Med. Chem. Lett.* **2003**, *13*, 51−55.
(51) Barbazán, P.; Carballo, R.; Vázquez-López, E. M. Synthesis and structure of acetylpyridine-salicyloylhydrazone and its copper(II) and zinc(II) complexes. The effect of the metal coordination on the weak intermolecular interactions. *Cryst. Eng. Commun.* **2007**, *9*, 668−675.
(52) Bakir, M.; Brown, O. Molecular structure and optosensing behaviour of di-2-pyridyl ketone benzoylhydrazone in non-aqueous solvents. *J. Mol. Struct.* **2002**, *609*, 129−136.
(53) Bernhardt, P. V.; Caldwell, L. M.; Chaston, T. B.; Chin, P.; Richardson, D. R. Cytotoxic iron chelators: characterization of the structure, solution chemistry and redox activity of ligands and iron complexes of the di-2-pyridyl ketone isonicotinoyl hydrazone (HPKIH) analogues. *JBIC, J. Biol. Inorg. Chem.* **2003**, *8*, 866−880.
(54) Bernhardt, P. V.; Wilson, G. J.; Sharpe, P. C.; kalinowski, D. S.; Richardson, D. R. Tuning the antiproliferative activity of biologically active iron chelators: characterization of the coordination chemistry and biological efficacy of 2-acetylpyrodine and 2-benzoylpyridine hydrazone ligands. *JBIC, J. Biol. Inorg. Chem.* **2008**, *13*, 107−119.
(55) Despaigne, A. A. R.; Parrilha, G. L.; Izidoro, J. B.; da Costa, P. R.; dos Santos, R. G.; Piro, O. E.; Castellano, E. E.; Rocha, W. R.; Beraldo, H. 2-Acetylpyridine- and 2-benzoylpyridine-derived hydrazones and their gallium(III) complexes are highly toxic to glioma cells. *Eur. J. Med. Chem.* **2012**, *50*, 163−172.
(56) Piló, E. D.; Recio-Despaigne, A. A.; Da Silva, J. G.; Ferreira, I. P.; Takahashi, J. A.; Beraldo, H. Effect of coordination to antimony(III) on the antifungal activity of 2-acetylpyridine- and 2-benzoylpyridine-derived hydrazones. *Polyhedron* **2015**, *97*, 30−38.
(57) You, Z.; Yu, H.; Li, Z.; Zhai, W.; Jiang, Y.; Li, A.; Guo, S.; Li, K.; Lv, C.; Zhang, C. Inhibition strudies of jack bean urease with hydrazones and their copper(II) complexes. *Inorg. Chim. Acta* **2018**, *480*, 120−126.
(58) Fousiamol, M. M.; Sithambaresan, M.; Damodaran, K. K.; Kurup, M. R. P. Syntheses, spectral aspects and biological studies of bromide and azide bridged box dimer copper(II) complexes of an NNO donor aroylhydrazone. *Inorg. Chim. Acta* **2020**, *501*, No. 119301.
(59) Santos, A. F.; Ferreira, I. P.; takahashi, J. A.; Rodrigues, G. L. S.; Pinheiro, C. B.; Teixeira, L. R.; Rocha, W. R.; Beraldo, H. Silver(I) complexes with 2-acetylpyridinebenzoylhydrazones exhibit antimicrobial effects against yeast and filamentous fungi. *New J. Chem.* **2018**, *42*, 2125−2132.
(60) Barbazán, P.; Carballo, R.; Prieto, I.; Turnes, M.; Vázquez-López, E. M. Synthesis, and characterization of several rhenium(I) complexes of 2-acetylpyridine and ferrocenyl carbaldehyde derivatives of 2-hydroxybenzoic acid hydrazide. *J. Organomet. Chem.* **2009**, *694*, 3102−3111.
(61) Despaigne, A. A. R.; Da Silva, J. G.; do Carmo, A. C. M.; Piro, O. E.; Castellano, E. E.; Beraldo, H. Structural studies on zinc(II) complexes with 2-benzoylpyridine-derived hydrazones. *Inorg. Chim. Acta* **2009**, *362*, 2117−2122.

https://doi.org/10.1021/acsomega.5c01984
ACS Omega 2025, 10, 23440−23460

(62) Despaigne, A. A. R.; Vieira, L. F.; Mendes, I. C.; da Costa, F. B.; Speziali, N. L.; Beraldo, H. Organotin(IV) complexes with 2-acetylpyridine benzoyl hydrazones: antimicrobial activity. *J. Braz. Chem. Soc.* **2010**, *21*, 1247−1257.
(63) Kant, R.; Yang, M.-H.; Tseng, C.-H.; Yen, C.-H.; Li, W.-Y.; Tyan, Y.-C.; Chen, M.; Tzeng, C.-C.; Chen, W.-C.; You, K.; Wang, W.-C.; Chen, Y.-L.; Chen, Y.-M. A. Discovery of an orally efficacious,MCY inhibitor for liver cancer using a GNMT-based high-throughput screening system and structure-activity relationship analysis. *J. Med. Chem.* **2021**, *64*, 8992−9009.
(64) Kang, S.; Shiota, Y.; Kariyazaki, A.; Kanegawa, S.; Yoshizawa, K.; Sato, O. Heterometallic Fe^{III}/K coordination polymer with a wide thermal hysteretic spin transition at room temperature. *Chem. - Eur. J.* **2016**, *22*, 532−538.
(65) Kovala-Demertzi, D.; Yadav, P. N.; Demertzis, M. A.; Jasiski, J. P.; Andreadaki, F. J.; Kostas, I. D. First use of a palladium complex with a thiosemicarbazone ligand as catalyst precursor for the Heck reaction. *Tetrahedron Lett.* **2004**, *45*, 2923−2926.
(66) Langeslay, R. R.; Kaphan, D. M.; Marshall, C. M.; Stair, P. C.; Sattelberger, A. P.; Delferro, M. Catalytic applications of vanadium: a mechanistic perspective. *Chem. Rev.* **2019**, *119*, 2128−2191.
(67) Jungwirth, U.; Kowol, C. R.; Keppler, B. K.; Hartinger, C. G.; Berger, W.; Heffeter, P. Anticancer Activity of Metal Complexes: Involvement of Redox Processes. *Antioxid. Redox Signal.* **2011**, *15*, 1085−1127.
(68) Mohan, B.; Chaudhary, M. Synthesis, crystal structure, computational study and anti-virus effect of mixed ligand copper(II) complex with ONS donor Schiff base and 1,10-phenanthroline. *J. Mol. Struct.* **2021**, *1246*, No. 131246.
(69) Ambalavanan, P.; Palani, K.; Ponnuswamy, M. N. Crystal structure of [1-(2-phenyloxyN[N-cyclohexylthiouryl)] ethylamine-(1,10-phenanthrolinyl)]copper(II). *Cryst. Res. Technol.* **2002**, *37*, 1249−1254.
(70) Naik, A. D.; Reddy, P. A. N.; Nethaji, M.; Chakravarty, A. R. Ternary copper(II) complexes of thiosemicarbazones and heterocyclic bases showing N_3OS coordination as models for the type-2 centers of copper monooxygenases. *Inorg. Chim. Acta* **2003**, *349*, 149−158.
(71) Thomas, A. M.; Naik, A. D.; Nethaji, M.; Chakravarty, A. R. Synthesis, crystal structure and photo-induced DNA cleavage activity of ternary copper(II)-thiosemicarbazone complexes having heterocyclic bases. *Inorg. Chim. Acta* **2004**, *357*, 2315−2323.
(72) Lobana, T. S.; Indoria, S.; Jassal, A. K.; Kaur, H.; Arora, D. S.; Jasinski, J. P. Synthesis, structures, spectroscopy and antimicrobial properties of complexes of copper(II) with salicylaldehyde N-substituted thiosemicarbazones and 2,2′-bipyridine or 1,10-phenanthroline. *Eur. J. Med. Chem.* **2014**, *76*, 145−154.
(73) Indoria, S.; Lobana, T. S.; Kauer, H.; Arora, D. S.; Randhawa, B. S.; Jassal, A. K.; Jasinski, J. P. Synthesis and structures of 5-methoxysalicyladehyde thiosemicarbazonates of copper(II): molecular spectroscopy, ESI-mass studies and antimicrobial activity. *Polyhedron* **2016**, *107*, 9−18.
(74) Lobana, T. S.; Indoria, S.; Sood, S.; Arora, D. S.; Randhawa, B. S.; Garcia-Santos, I.; Smolinski, V. A.; Jasinski, J. P. Synthesis of 5-nitrosalicylaldehyde-N-substituted thiosemicarbazonates of copper-(II): molecular structures, spectroscopy, ESI-mass studies and antimicrobial activity. *Inorg. Chim. Acta* **2017**, *461*, 248−260.
(75) Ainscough, E. W.; Brodie, A. M.; Ranford, J. D.; Waters, J. M. Reaction of nitrogen and sulphur donor ligands with the antitumour complex $[\{CuL(MeCO_2)\}_2]$ (HL = 2-formylpyridine thiosemicarbazone) and the single-crystal X-ray structureof $[CuL(bipy)]ClO_4$ (bipy = 2,2′-bipyridine). *J. Chem. Soc., Dalton Trans.* **1991**, 1737−1742.
(76) Kartikeyan, R.; Murugan, D.; Ajaykamal, T.; Varadhan, M.; Rangasamy, L.; Velusamy, M.; Palaniandavar, M.; Rajendiran, V. Mixed ligand copper(II)-diimine complexes of 2-formylpyridine-N^4-phenylthiosemicarbazone: diimine co-ligands tune the *in vitro* nanomolar cytotoxicity. *Dalton Trans.* **2023**, *52*, 9148−9169.
(77) Sreeja, P. B.; Kurup, M. R. P.; Kishore, A.; Jasmin, C. Spectral characterization, X-ray structure and biological investigations of copper(II) ternary complexes of 2-hydroxyacetophenone 4-hydroxybenzoic acid hydrazone and heterocyclic bases. *Polyhedron* **2004**, *23*, 575−581.
(78) Reddy, P. A. N.; Santra, B. K.; Nethji, M.; Chakravarty, A. R. Metal-assisted light-induced DNA cleavage activity of 2-(methylthio)-phenylsalicyladimine Shiff base copper(II) complexes having planar heterocyclic bases. *J. Inorg, Biochem.* **2004**, *98*, 377−386.
(79) Reddy, P. R.; Shilpa, A.; Raju, N.; Raghavaiah, P. Synthesis, structure, DNA binding and cleavage properties of ternary amino acid Schiff base-phen/bipy Cu(II) complexes. *J. Inorg. Biochem.* **2011**, *105*, 1603−1612.
(80) Li, A.; Liu, Y.-H.; Yuan, L.-Z.; Ma, Z.-Y.; Zhao, C.-L.; Xie, C.-Z.; Bao, W.-G.; Xu, J.-Y. Association of structural modifications with bioactivity in three new copper(II) complexes of Schiff base ligands derived from 5-chlorosalicylaldehyde and amino acids. *J. Inorg. Biochem.* **2015**, *146*, 52−60.
(81) Rajendiran, V.; Karthik, R.; Palaniandavar, M.; Stoeckli-Evans, H.; Periasamy, V. S.; Akbarsha, M. A.; Srinag, B. S.; Krishnamurthy, H. Mixed-ligand copper(II)-phenolate complexes: effect of coligand on enhanced DNA and protein binding, DNA cleavage, and anticancer activity. *Inorg. Chem.* **2007**, *46*, 8208−8221.
(82) Reddy, P. A. N.; Nethaji, M.; Chakravarty, A. R. Synthesis, crystal structures and properties of ternary copper(II) complexes having 2,2′-bipyridine and amino acid salicylaldiminates as models for the type-2 sites in copper oxidases. *Inorg. Chim. Acta* **2002**, *337*, 450−458.
(83) Mathew, N.; Sithambaresan, M.; Kurup, M. R. P. Spectral studies of copper(II) complexes of tridentate acylhdrazone ligands with heterocyclic compounds as coligands: X-ray crystal structure of one acylhydrazone copper(II) complex. *Spectrochim. Acta, Part A* **2011**, *79*, 1154−1161.
(84) Koh, L. L.; Ranford, J. O.; Robinson, W. T.; Svensson, J. O.; Tan, A. L. C.; Wu, D. Model for the reduced Schiff base intermediate between amino acids and pyridoxal: copper(II) complexes of *N*-(2-hdroxybenzyl)amino acids with nonpolar side chains and the crystal structures of [Cu(*N*-(2-hydroxybenzyl)-D,L-alanine)(phen·H_2O and [Cu(*N*-(2-hydroxybenzyl)-D,L-alanine)(imidazole)]. *Inorg. Chem.* **1996**, *35*, 6466−6472.
(85) Bernal, M.; García-Vázquez, J. A.; Romero, J.; Gómez, C.; Durán, M. L.; Sousa, A.; Sousa-Pedrares, A.; Rose, D. J.; Maresca, K. P.; Zubieta, J. Electrochemical synthesis of cobalt, nickel, zinc and cadmium complexes with *N*[(2-hydroxyphenyl)methylidine]-*N*′-tosylbenzene-1,2-diamine. The crystal structures of {1,10-phenanthroline)[*N*-2-oxophenyl)methylidine]-*N*-tosylbenzene-1,2-diaminato}nickel(II) and {1,10-phenanthroline)[*N*-2-oxophenyl)-methylidine]-*N*′-tosylbenzene-1,2-diaminato}copper(II). *Inorg. Chim. Acta* **1999**, *295*, 39−47.
(86) Wang, M.-Z.; Meng, Z.-X.; Liu, B. L.; Cai, G.-L.; Zhang, C.-L.; Wang, X.-Y. Novel tumor chemotherapeutic agents and tumor radio-imaging agents: potential tumor pharmaceuticals of ternary copper(II) complexes. *Inorg. Chem. Commun.* **2005**, *8*, 368−371.
(87) Reddy, P. A. N.; Nethaji, M.; Chakravarty, A. R. Hydrolytic cleavage of DNA by ternary amino acid Schiff base copper(II) complexes having planar heterocyclic ligands. *Eur. J. Inorg. Chem.* **2004**, *2004*, 1440−1446.
(88) Dong, J.; Li, L.; Liu, G.; Xu, T.; Wang, D. Synthesis, crystal structure and DNA-binding properties of a new copper(II) complex with L-valine Schiff base and 1,10-phenanthroline. *J. Mol. Struct.* **2011**, *986*, 57−63.
(89) Labisbal, E.; Garcia-Vazquez, J. A.; Romero, J.; Picos, S.; Sousa, A.; Castiñeiras, A.; Maichle-Mössmer, C. Electrochemical synthesis and structural characterization of nickel(II) and copper(II) complexes of tridentate Schiff bases: molecular structure and the five-coordinated copper(II) complex: 1,10-phenanthroline {2-[2-oxyphenyl)-iminomethyl]phenolato}copper(II). *Polyhedron* **1995**, *14*, 663−670.
(90) Sharma, M.; Ganeshpandian, M.; Majumder, M.; Tamilarasan, A.; Sharma, M.; Mukhopadhyay, R.; Islam, N. S.; Palaniandavar, M. Octahedral copper(II)-diimine complexes of triethylenetetramine: effect of stereochemical fluxionality and ligand hydrophobicity on

https://doi.org/10.1021/acsomega.5c01984
ACS Omega 2025, 10, 23440−23460

Cu^{II}/Cu^{I} redox, DNA binding and cleavage, cytotoxicity and apoptosis-inducing ability. *Dalton Trans.* **2020**, *49*, 8282−8297.
(91) Ng, C. H.; Kong, K. C.; Von, S. T.; Balraj, P.; Jensen, P.; Thirthagiri, E.; Hamada, H.; Chikira, M. Synthesis, characterization, DNA-binding study and anticancer properties of ternary metal(II) complexes of edda and an intercalating ligand. *Dalton Trans.* **2008**, 447−454.
(92) Selvakumar, B.; Rajendiran, V.; Maheswari, P. U.; Stoeckli-Evans, H.; Palaniandavar, M. Structures, spectra, and DNA-binding properties of mixed ligand copper(II) complexes of iminodiacetic acid: the novel role of diamine co-ligands on DNA conformation and hydrolytic and oxidative double strand DNA cleavage. *J. Inorg. Biochem.* **2006**, *100*, 316−330.
(93) Yang, C.-T.; Moubaraki, B.; Murray, K. S.; Vittal, J. J. Synthesis, characterization and properties of ternary copper(II) complexes containing reduced Schiff base *N*-(2-hdroxybenzyl)-amino acids and 1,10-phenanthroline. *Dalton Trans.* **2003**, 880−889.
(94) Yang, C. T.; Moubaraki, B.; Murray, K. S.; Ranford, J. D.; Vittal, J. J. Interconversion of a monomer and two coordination polymers of a copper(II)-reduced Schiff base ligand-1,10-phenanthroline complex based on hydrogen- and coordinative-bonding. *Inorg. Chem.* **2001**, *40*, 5934−5941.
(95) Reddy, P. A. N.; Nethaji, M.; Chakravarty, A. R. Ternary mononuclear and ferromagnetically coupled dinuclear copper(II) complexes of 1,10-phenanthroline and *N*-salicylidine-2-methoxyaniline that show supramolecular self-organization. *Eur. J. Inorg. Chem.* **2003**, *2003*, 2318−2324.
(96) Yuan, C.; Lu, L.; Gao, X.; Wu, Y.; Guo, M.; Li, Y.; Fu, X.; Zhu, M. Ternary oxovanadium(IV) complexes of ONO-donor Schiff base and polypyridyl derivatives as protein tyrosine phosphatase inhibitors: synthesis, characterization, and biological activities. *JBIC, J. Biol. Inorg. Chem.* **2009**, *14*, 841−851.
(97) (a) Banerjee, S.; Dixit, A.; Shridharan, R. N.; Karande, A. A.; Chakravarty, A. R. Endoplasmic reticulum targeted chemotherapeutics: the remarkable photo-cytotoxicity of an oxovanadium(IV) vitamin-B6 complex in visible light. *Chem. Commun.* **2014**, *50*, 5590−5592. (b) Banerjee, S.; Dixit, A.; Karande, A. A.; Chakravarty, A. R. Endoplasmic reticulum targeting tumour selective photocytotoxic oxovanadium(IV) complexes having vitamin-B6 and acridinyl moieties. *Dalton Trans.* **2016**, *45*, 783−796. (c) Sasmal, P. K.; Patra, A. K.; Nethaji, M.; Chakravarty, A. R. DNA cleavage by new oxovanadium(IV) complexes of *N*-salicylidene α-amino acids and phenanthroline bases in the photodynamic therapy window. *Inorg. Chem.* **2007**, *46*, 11112−11121.
(98) Dutta, S. K.; Tiekink, E. R. T.; Chaudhury, M. Mono- and dinuclear oxovanadium(IV) compounds containing VO(ONS) basic core: synthesis, structure and spectroscopic properties. *Polyhedron* **1997**, *16*, 1863−1871.
(99) Jang, Y. J.; Lee, U.; Koo, B. K. Oxovanadium(IV) complexes containing VO(ONS) basic core: synthesis, structure and spectroscopic properties. *Bull. Korean Chem. Soc.* **2005**, *26*, 72−76.
(100) Geary, W. J. The use of conductivity measurements in organic solvents for the characterisation of coordination compounds. *Coord. Chem. Rev.* **1971**, *7*, 81−122.
(101) Bastos, A. M. B.; da Silva, J. G.; Maia, P. I. S.; Deflon, V. M.; Batista, A. A.; Ferreira, A. V. M.; Botion, L. M.; Niquet, E.; Beraldo, H. Oxovanadium(IV) and (V) complexes of acetylpyridine-derived semicarbazones exhibit insulin-like activity. *Polyhedron* **2008**, *27*, 1787−1794.
(102) Saswati; Adão, S.; majumder, S.; Dash, S. P.; Roy, S.; Kuznetsov, M. L.; Pessoa, J. C.; Gomes, G. S. B.; Hardikar, M. R.; Tiekink, E. R. T.; Dinda, R. Synthesis, Structure, solution behavior, reactivity and biological evaluation of oxidovanadium(IV/V) thiosemicarbazone complexes. *Dalton Trans.* **2018**, *47*, 11358−11374.
(103) Molter, A.; Bill, E.; Mohr, F. Synthesis, structures and reactivity of two oxidovanadium(IV) and dioxidovanadium(V) selenosemicarbazonato complexes. *Inorg. Chem. Commun.* **2012**, *17*, 124−127.
(104) Maia, P. I. S.; Pavan, F. R.; Leite, C. Q. F.; Lemos, S. S.; de Sousa, G. F.; Batista, A. A.; Nasciemento, O. R.; Ellena, J.; Castellano, E. E.; Niquet, E.; Deflon, V. M. Vanadium complexes with thiosemicarbazones: synthesis, characterization, crystal structures and anti-*Mycobecterium tuberculosis* activity. *Polyhedron* **2009**, *28*, 398−406.
(105) Kowol, C. R.; Nagy, N. V.; Jakusch, T.; Roller, A.; Heffeter, P.; Keppler, B. K.; Enyedy, E. A. vanadium(IV/V) complexes of Triapine and related thiosemicarbazones: synthesis, solution, equilibrium and bioactivity. *J. Inorg. Biochem.* **2015**, *152*, 62−73.
(106) Ghorbanloo, M.; Bikas, R.; Jafari, S.; Krawcyzk, M. S.; Lis, T. Synthesis, structural characterization and catalytic potential of oxidovanadium(IV) and dioxovanadium(V) complexes with thiazole-derived NNN-donor ligand. *J. Coord. Chem.* **2018**, *71*, 1510−1525.
(107) Sarkar, A.; Pal, S. Some ternary complexes of oxovanadium-(IV) with acetylacetone and *N*-(2-pyridyl)-*N*′-(salicylidene)hydrazine and its derivatives. *Polyhedron* **2006**, *25*, 1689−1694.
(108) Shongwe, M. S.; Al-Barhi, K. S.; Mikuriya, M.; Adams, H.; Morris, M. J.; Bill, E.; Molloy, K. C. Tuning a single ligand system to stabilize multiple spin states of manganese: a first example of a hydrazone-based manganese(III) spin-crossover complex. *Chem. - Eur. J.* **2014**, *20*, 9693−9701.
(109) Shongwe, M. S.; Al-Rahbi, S. H.; Al-Azani, M. A.; Al-Muharbi, A. A.; Al-Mjeni, F.; Matoga, D.; Gismelseed, A.; Al-Omari, I. A.; Yousif, A.; Adams, H.; Morris, M. J.; Mikuriya, M. Coordination versatility of tridentate pyridyl aroylhydrazones towards iron: tracking down the elusive aroylhydrazono-based ferric spin-crossover molecular materials. *Dalton Trans.* **2012**, *41*, No. 25002514.
(110) Shongwe, M. S.; Al-Zaabi, U.; Al-Mjeni, F.; Eribal, C. S.; Sinn, E.; Al-Omari, I. A.; Hamdeh, H. H.; Matoga, D.; Adams, H.; Morris, M. J.; Rheingold, A. L.; Bill, E.; Sellmyer, D. J. Accessibility and selective stabilization of the principal spin states of iron by pyridyl versus phenolic ketimines: modulation of the $^{6}A_1 \leftrightarrow {}^{2}T_2$ ground-state transformation of the $[FeN_4O_2]^+$ chromophore. *Inorg. Chem.* **2012**, *51*, 8241−8253.
(111) Al-Azzani, M. A.; Al-Mjeni, F.; Mitsuhashi, R.; Mikuriya, M.; Al-Omari, I. A.; Robertson, C. C.; Bill, E.; Shongwe, M. S. Unusual magneto-structural features of the halo-substituted materials $[Fe^{III}(5\text{-X-salMeen})_2Y$: a cooperative [HS-HS]↔[HS-LS] spin transition. *Chem. - Eur. J.* **2020**, *26*, 4766−4779.
(112) Thakur, S.; Drew, M. G. B.; Franconetti, A.; Frontera, A.; Chattopadhyay, S. Analysis of energies of halogen and hydrogen bonding interactions in the solid state structures of vanadyl Schiff base complexes. *RSC Adv.* **2019**, *9*, 4789−4796.
(113) Noblía, P.; Vieites, M.; Parajón-Costa, B. S.; Baran, E. J.; Cerecetto, H.; Draper, P.; González, M.; Piro, O. E.; Castellano, E. E.; Azqueta, A.; de Ceráin, A. L.; Monge-Vega, A.; Gambino, D. Vanadium(V) complexes with salicylaldehyde semicarbazone derivatives bearing in vitro anti-tumor activity toward kidney tumor cells (TK-10): crystal structure of $[V^{V}O_2$(5-bromosalicyladehyde semicarbazone)]. *J. Inorg. Biochem.* **2005**, *99*, 443−451.
(114) Maurya, M. R.; Kumar, A.; Bhat, A. R.; Azam, A.; Bader, C.; Rehder, D. Dioxo- and oxovanadium(IV) complexes of thiohydrazone ONS donor ligands: synthesis, characterization, reactivity, and antiamoebic activity. *Inorg. Chem.* **2006**, *45*, 1260−1269.
(115) Asgedom, G.; Sreedhara, A.; Kivikoski, J.; Valkonen, J.; Kolehmainen, E.; Rao, C. P. Alkoxo, bound monooxo- and dioxovanadium(V) complexes: synthesis, characterization, X-ray crystal structures, and solution reactivity studies. *Inorg. Chem.* **1996**, *35*, 5674−5683.
(116) Maurya, M. R.; Khurana, S.; Zhang, W.; Rehder, D. Vanadium(IV/V) complexes containing $[VO]^{2+}$, $[VO]^{3+}$, $[VO_2]^+$ and $[VO)O_2)]^+$ cores with ligands derived from 2-acetylpyridine and *S*-benzyl- or *S*-methyldithiocarbazate. *Eur. J. Inorg. Chem.* **2002**, *2002*, 1749−1760.
(117) Philip, V.; Manoj, E.; Kurup, M. R. P.; Nethaji, M. [Di-2-pyridyl ketone N^4,N^4-(butane-1,4-diyl)thiosemicarbazonato-

https://doi.org/10.1021/acsomega.5c01984
ACS Omega 2025, 10, 23440−23460

$\kappa^3N,N'S$]dioxovanadium(V). *Cryst. Struct. Commun.* **2005**, *C61*, m488−m490.
(118) Shongwe, M. S.; Al-Kharousi, H. N. R.; Adams, H.; Morris, M. J.; Bill, E. Unprecedented $[V_2O]^{6+}$ Core of a centrosymmetric thiosemicarbazonato dimer: spontaneous deoxygenation of oxovanadium(IV). *Inorg. Chem.* **2006**, *45*, 1103−1107.
(119) Addison, A. W.; Rao, T. N.; Reedijk, J.; van Rijn, J.; Verschoor, G. C. Synthesis, structure, and spectroscopic properties of copper(II) compounds containing nitrogen-sulphur donor ligands: the crystal and molecular structure of aqua[1,7-bis(N-methylbenzimidazol-2′-yl)-2,6-dithiaheptane]copper(II) perchlorate. *J. Chem. Soc., Dalton Trans.* **1984**, 1349−1356.
(120) Anderson, O. P. Crystal and molecular structure of tris-(1,10-phenanthroline)copper(II) perchlorate. *J. Chem. Soc., Dalton* **1973**, 1237−1241.
(121) Burčák, M.; Potočňák, I.; Baran, P.; Jäger, L. Low-dimensional compounds containing cyano groups. X. (Dicyanamido-κN^1)bis(1,10-phenanthroline-κ^2N,N')copper(II) perchlorate. *Cryst. Struct. Commun.* **2004**, *60*, m601−m604.
(122) Bernhardt, P. V.; Sharpe, P. C.; Islam, M.; Lovejoy, D. B.; Kalinowski, D. S.; Richardson, D. R. Iron chelators, of the dipyridylketone thiosemicarbazone class: precomplexation, and transmetalation effects on anticancer activity. *J. Med. Chem.* **2009**, *52*, 407−415.
(123) Sreekanth, A.; Sivakumar, S.; Kurup, M. R. P. Structural studies of six and four coordinate zinc(II), nickel(II) and dioxovanadium(V) complexes with thiosemicarbazones. *J. Mol. Struct.* **2003**, *655*, 47−58.
(124) Mendes, I. C.; Botion, L. M.; Ferreira, A. V. M.; Castellano, E. E.; Beraldo, H. Vanadium complexes with 2-pyridineformamide thiosemicarbazones: *In vitro* studies of insulin-like activity. *Inorg. Chim. Acta* **2009**, *362*, 414−420.
(125) Mendes, I. C.; Speziali, N. L.; Beraldo, H. Dioxido{1-[(phenyl)(2-pyridyl)methylene]-4-(*p*-tolyl)thiosemicarbazonato}-vanadium(V) dimethyl sulfoxide solvate. *Acta Cryst.* **2007**, *63*, No. m2391.
(126) Siqueira, J. D.; Menagatti, A. C. O.; Terenzi, H.; Pereira, M. B.; Roman, D.; Rosso, E. F.; Piquini, P. C.; Iglesias, B. A.; Back, D. F. Synthesis, characterization and phosphatase inhibitory activity of dioxidovanadium(V) complexes with Schiff base ligands derived from pyridoxal and resorcinol. *Polyhedron* **2017**, *130*, 184−194.
(127) Tei, L.; Blake, A. J.; Lippolis, V.; Wilson, C.; Schröder, M. Methanolysis of nitrile-functionalised pendant arm derivatives of 1,4,7-triazacyclononane upon coordination to Cu^{II}. *Dalton Trans.* **2003**, 304−310.
(128) Su, S.-Y.; Liao, S.; Wanner, M.; Fiedler, J.; Zhang, C.; Kang, B.-S.; Kaim, W. The copper(I)/copper(II) transition in complexes with 8-alkylthioquinoline based multidentate ligands. *Dalton Trans.* **2003**, 189−202.
(129) Tubbs, K. J.; Fuller, A. L.; Bennett, B.; Arif, A. M.; Makowska-Grzyska, M. M.; Berreau, L. M. Evaluation of the influence of a thioether substituent on the solid state and solution properties of N_3S-ligated copper(II) complexes. *Dalton Trans.* **2003**, 3111−3116.
(130) Maurya, M. R.; Khurana, S.; Shailendra; Azam, A.; Zhang, W.; Rehder, D. Synthesis, characterisation and antiamoebic studies of dioxovanadium(V) complexes containing ONS donor ligands derived from *S*-benzyldithiocarbazate. *Eur. J. Inorg. Chem.* **2003**, *2003*, 1966−1973.
(131) Maurya, M. R.; Khurana, S.; Zhang, W.; Rehder, D. Biomimetic oxo-, dioxo- and oxo-peroxo-hydrazonato-vanadium(IV/V) complexes. *J. Chem. Soc., Dalton Trans.* **2002**, 3015−3023.
(132) Dash, S. P.; Panda, A. K.; Pasayat, S.; Dinda, R.; Biswas, A.; Tiekink, E. R. T.; patil, Y. P.; Nethaji, M.; Kaminsky, W.; Mukhopadhyay, S.; Bhutia, S. K. Synthesis and structural investigation of some alkali metal ion-mediated $LV^VO_2^-$ (L^{2-} = tridentate ONO ligands) species: DNA binding, photoinduced DNA cleavage and cytotoxic activities. *Dalton Trans.* **2014**, *43*, 10139−10156.
(133) Plass, W.; Yozglatli, H.-P. Synthesis, reactivity, and structural characterization of dioxovanadioum(V) complexes with tridentate Schiff base ligand: vanadium complexes in supramolecular networks. *Z. Anor. Allg. Chem.* **2003**, *629*, 65−70.
(134) Asgedom, G.; Sreedhara, A.; Kivikoski, J.; Valkonen, J.; Kolehmainen, E.; Rao, C. P. Alkoxo bound monooxo- and dioxovanadium(V) complexes: synthesis, characterization, X-ray crystal structures, and solution reactivity studies. *Inorg. Chem.* **1996**, *35*, 5674−5683.
(135) Krivosudský, L.; Schwendt, P.; Gyepes, R.; Žák, Z. X-ray structure analysis, electronic and vibrational circular dichroismof chiral-at-metal dioxidovanadium(V) complexes with amino acids derived Schiff base ligands. *Polyhedron* **2014**, *81*, 421−427.
(136) Kwiatkowski, E.; Romanowski, G.; Nowicki, M.; Kwiatkowski, M.; Suwińska, K. Dioxovanadium(V) Schiff base complexes of *N*-methyl-1,2-diaminoethane and 2-methyl-1,2-diaminopropane with aromatic *o*-hydroxyaldehydes and *o*-hydroxyketones: synthesis, characterisation, catalytic properties and structure. *Polyhedron* **2003**, *22*, 1009−1018.
(137) Maurya, M. R.; Kumar, A.; Ebel, M.; Rehder, D. Synthesis, characterization, reactivity, and catalytic potential of model vanadium-(IV, V) complexes with benzimidazole-derived ONN donor ligands. *Inorg. Chem.* **2006**, *45*, 5924−5937.
(138) Maurya, M. R.; Bisht, M.; Kumar, A.; Kuznetsov, M. L.; Avecilla, F.; Pessoa, J. C. Synthesis, characterization, reactivity and catalytic activity of oxidovanadium(IV), oxidovanadium(V) and dioxidovanadium(V) complexes of benzimidazole modified ligands. *Dalton Trans.* **2011**, *40*, 6968−6983.
(139) Liu, Y. H.; Li, A.; Shao, J.; Xie, C.-Z.; Song, X.-Q.; Bao, W.-G.; Xu, J.-Y. Four Cu(II) complexes based on antitumour chelators: synthesis, structure, DNA binding/damage, HSA interaction and enhanced cytotoxicity. *Dalton Trans.* **2016**, *45*, 8036−8049.
(140) Ying, P.; Zeng, P.; Lu, J.; Chen, H.; Liao, X.; Yang, N. New oxidovanadium complexes incorporating thiosemicarbazones and 1,10-phenanthroline dervatives as DNA cleavage, potential anticancer agents, and hydroxyl radical scavenger. *Chem. Biol. Drug Des.* **2015**, *86*, 926−937.
(141) Ansari, K. I.; Grant, J. D.; Kasiri, S.; Woldermariam, G.; Shrestha, B.; Mandal, S. S. Manganese(III) salens induce tumpr selective apoptosis in human cells. *J. Inorg. Biochem.* **2009**, *103*, 818−826.
(142) Rowe, R. A.; Jones, M. M. Vanadium(IV) oxy(acetylacetone) [Bis(2,4-pentanediono) oxovanadium(IV)]. *Inorg. Synth.* **1957**, *5*, 113−116.
(143) *SADABS*; Bruker Axs Inc.: Madison, Wisconsin, USA, 2016.
(144) Krause, L.; Herbst-Irmer, R.; Sheldrick, G. M.; Stalke, D. Comparison of silver and molybdenum microfocus X-ray sources for single-crystal X-ray structure determination. *J. Appl. Crystallogr.* **2015**, *48*, 3−10.
(145) Sheldrick, G. M. SHELXT-integrated space-group and crystal-structure determination. *Acta Crystallogr., Sect. A:Found. Adv.* **2015**, *A71*, 3−8.
(146) Sheldrick, G. M. Crystal Structure Refinement with SHELXL. *Acta Crystallogr., Sect. C:Struct. Chem.* **2015**, *C71*, 3−8.
(147) Dolomanov, O. V.; Bourhis, L. J.; Gildea, R. J.; Howard, J. A. K. K.; Puschmann, H. OLEX2: a complete structure solution, refinement and analysis program. *J. Appl. Crystallogr.* **2009**, *42*, 339−341.

https://doi.org/10.1021/acsomega.5c01984
ACS Omega 2025, 10, 23440−23460